

# Coherence of Multi-Dimensional Pair Production Discharges in Polar Caps of Pulsars

Chernoglazov A., Philippov A., Timokhin A. 2024  
arXiv:2409.15409      Accepted by ApJL

Reporter: 曹顺顺  
(Shunshun Cao)

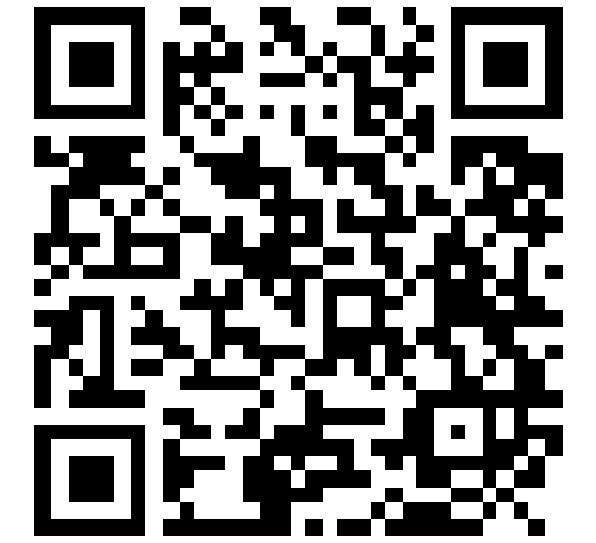
2024.10

27 pages in total

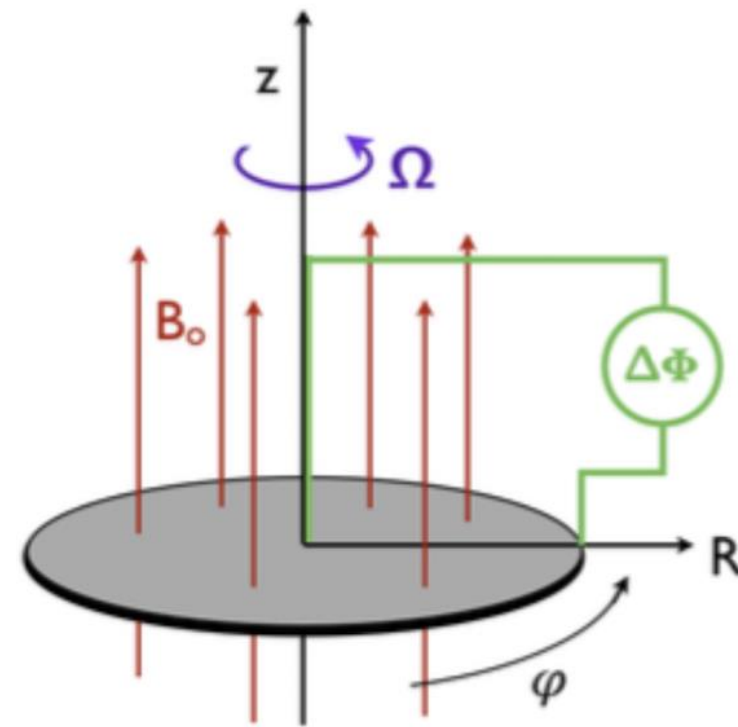


# I. Introduction

## (i) Pulsar magnetosphere and polar cap



A note in Zhihu  
for Amato's paper.

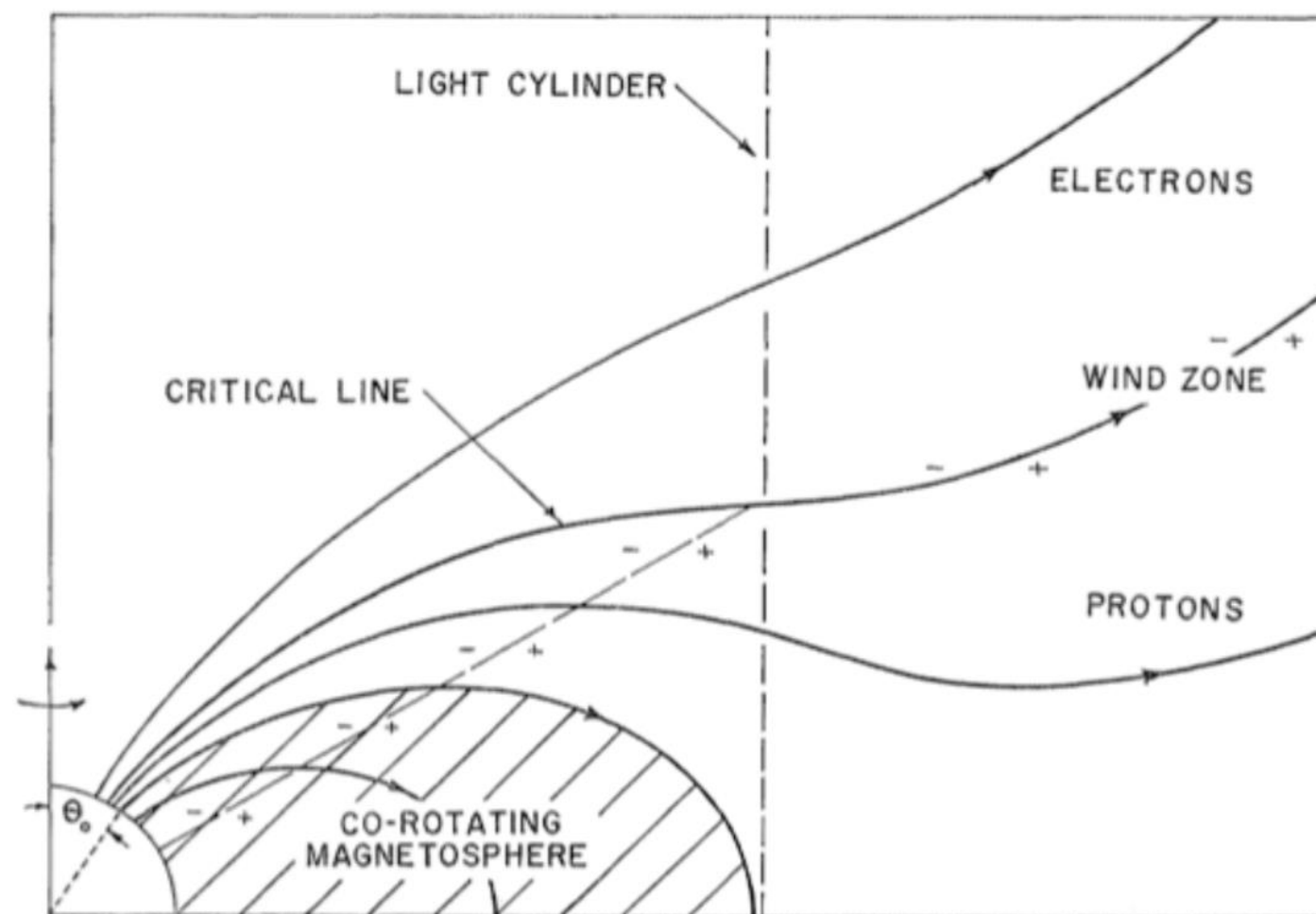


Pulsar  $\approx$  Faraday Disk

Rotating compact object in magnetic field

➔ Electric field distribution

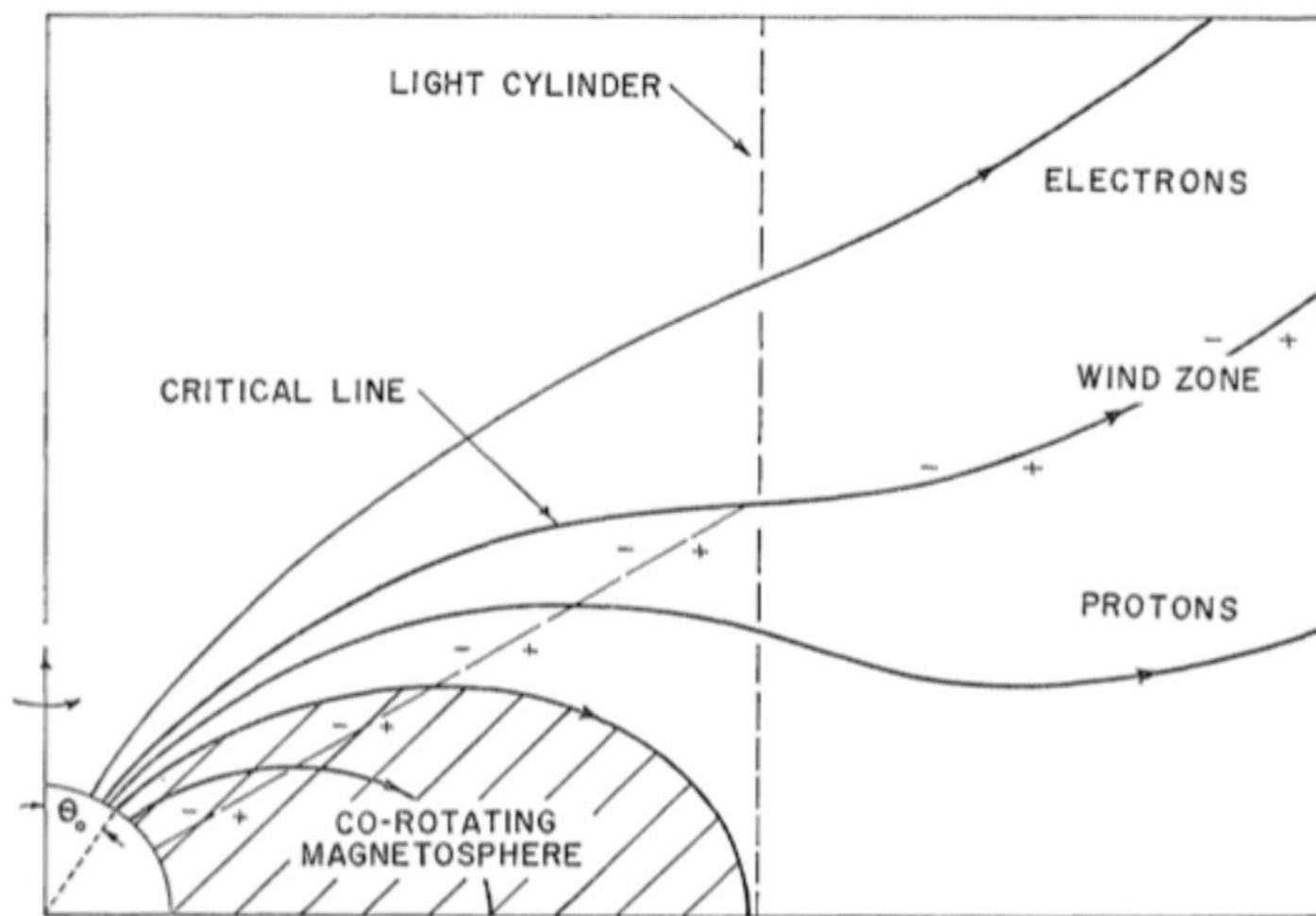
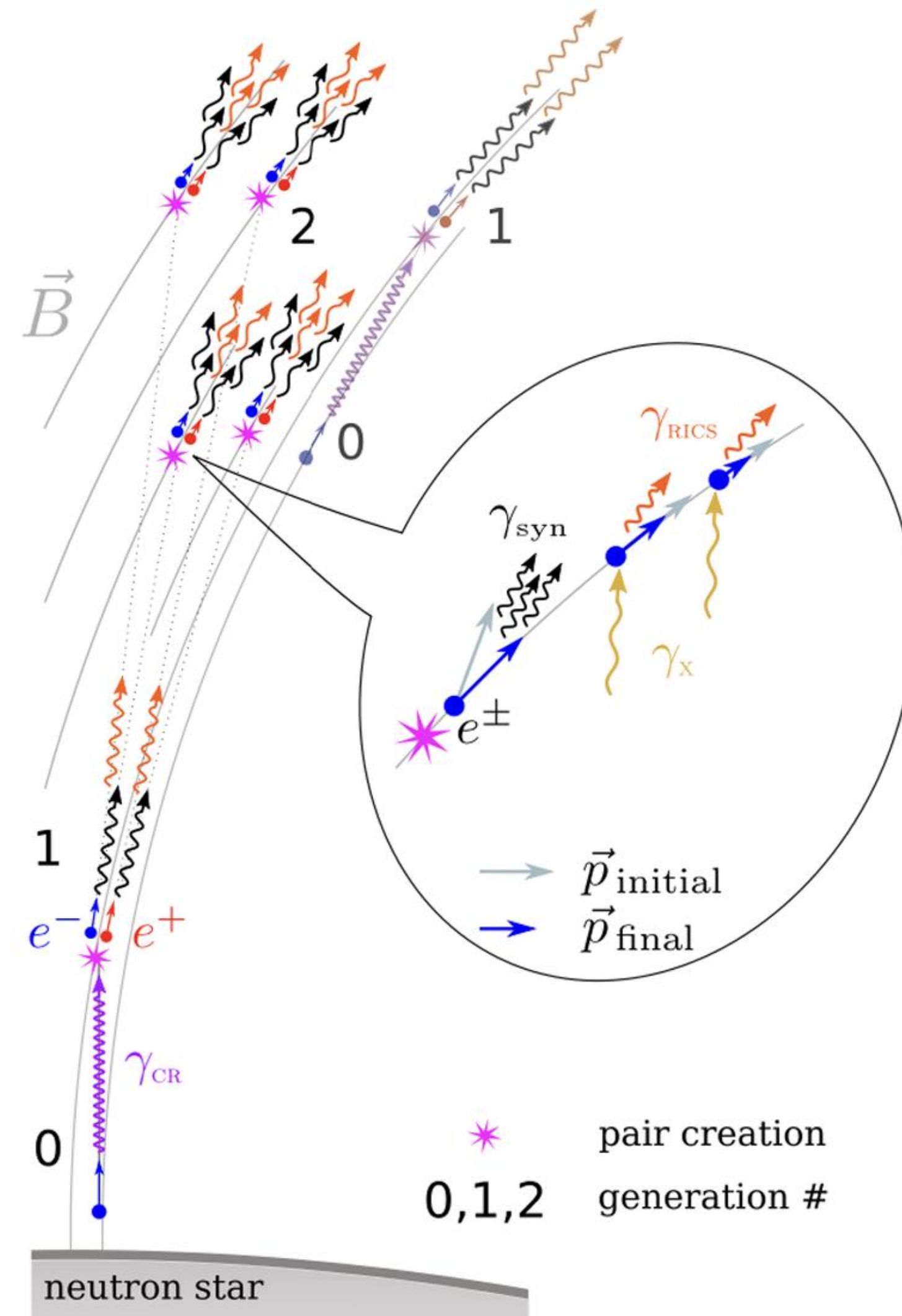
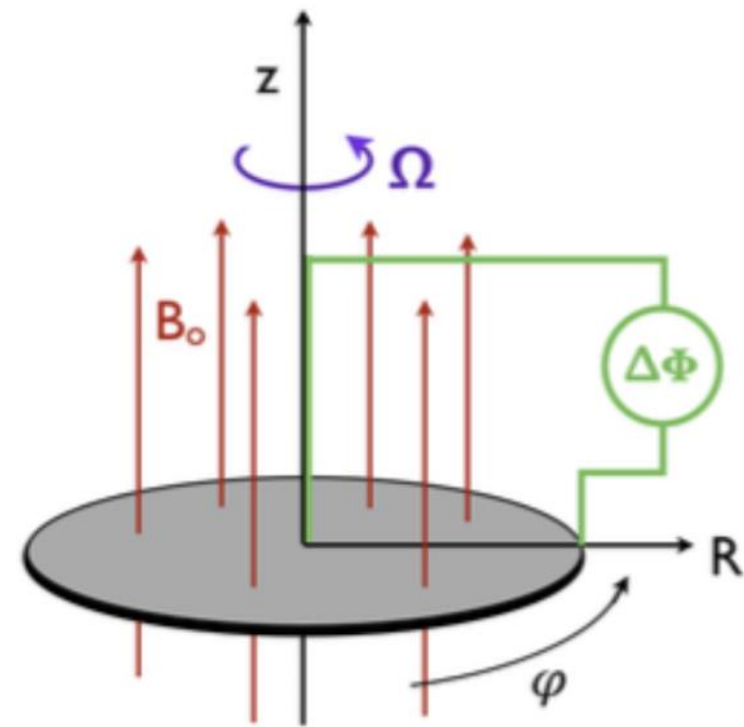
➔➔ Provide acceleration regions



Amato 2024 arxiv.



A note in Zhihu  
for Amato's paper.



- Initial particles in  $E$  field
- Accelerated particles
- Emitted photons  
(curvature or ICS)
- Pair ( $e^\pm$ ) creation
- Charge separation  
screen original  $E$  field

**(Discharge process)**

Amato 2024 arxiv.

Charged particles fill the pulsar surroundings → magnetized plasma → magnetosphere

Static magnetosphere:

$$q(\mathbf{E} + \mathbf{v} \times \mathbf{B}) = 0$$

Corotation condition:

$$\mathbf{E} + (\boldsymbol{\Omega} \times \mathbf{r}) \times \mathbf{B} = 0$$

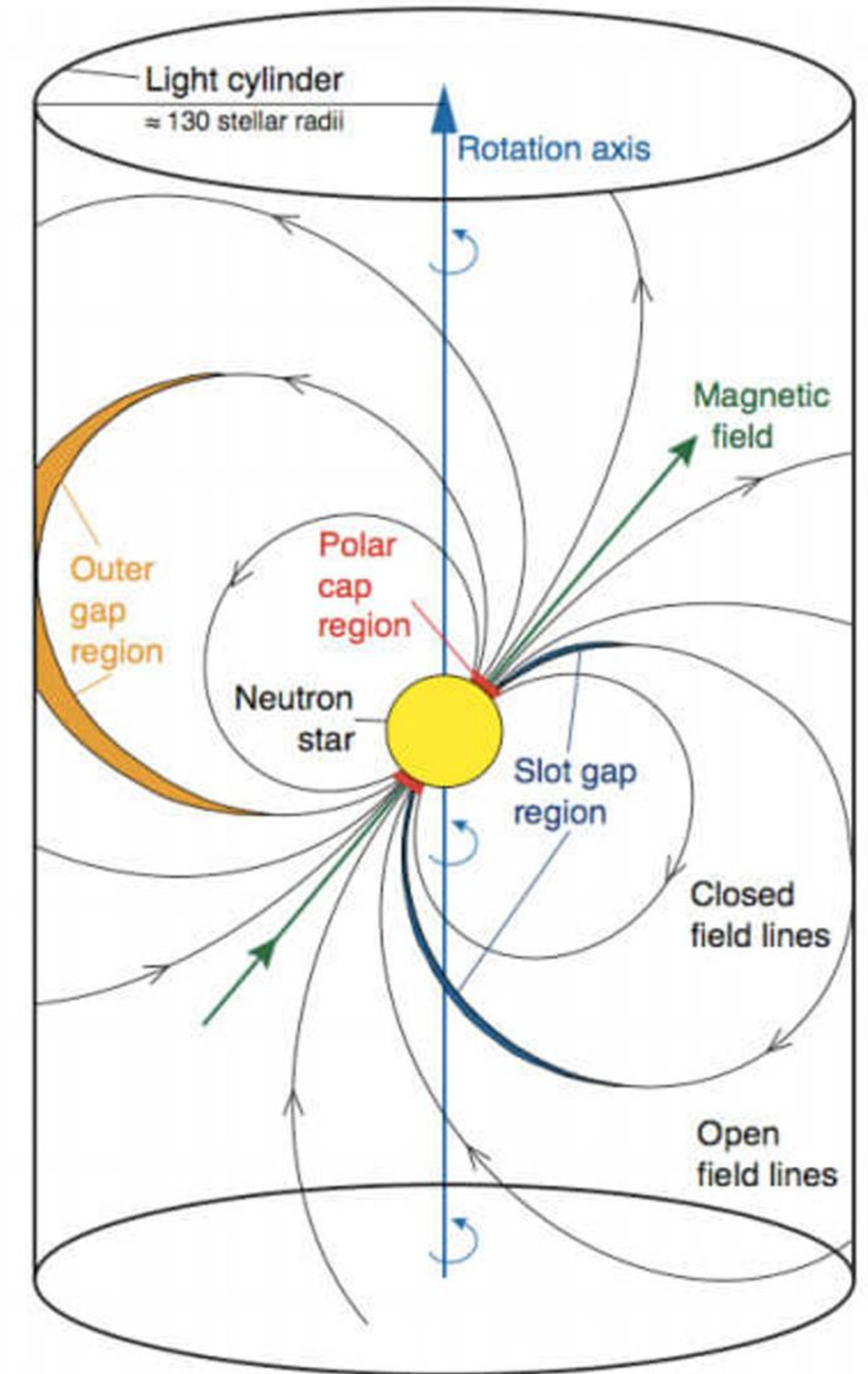
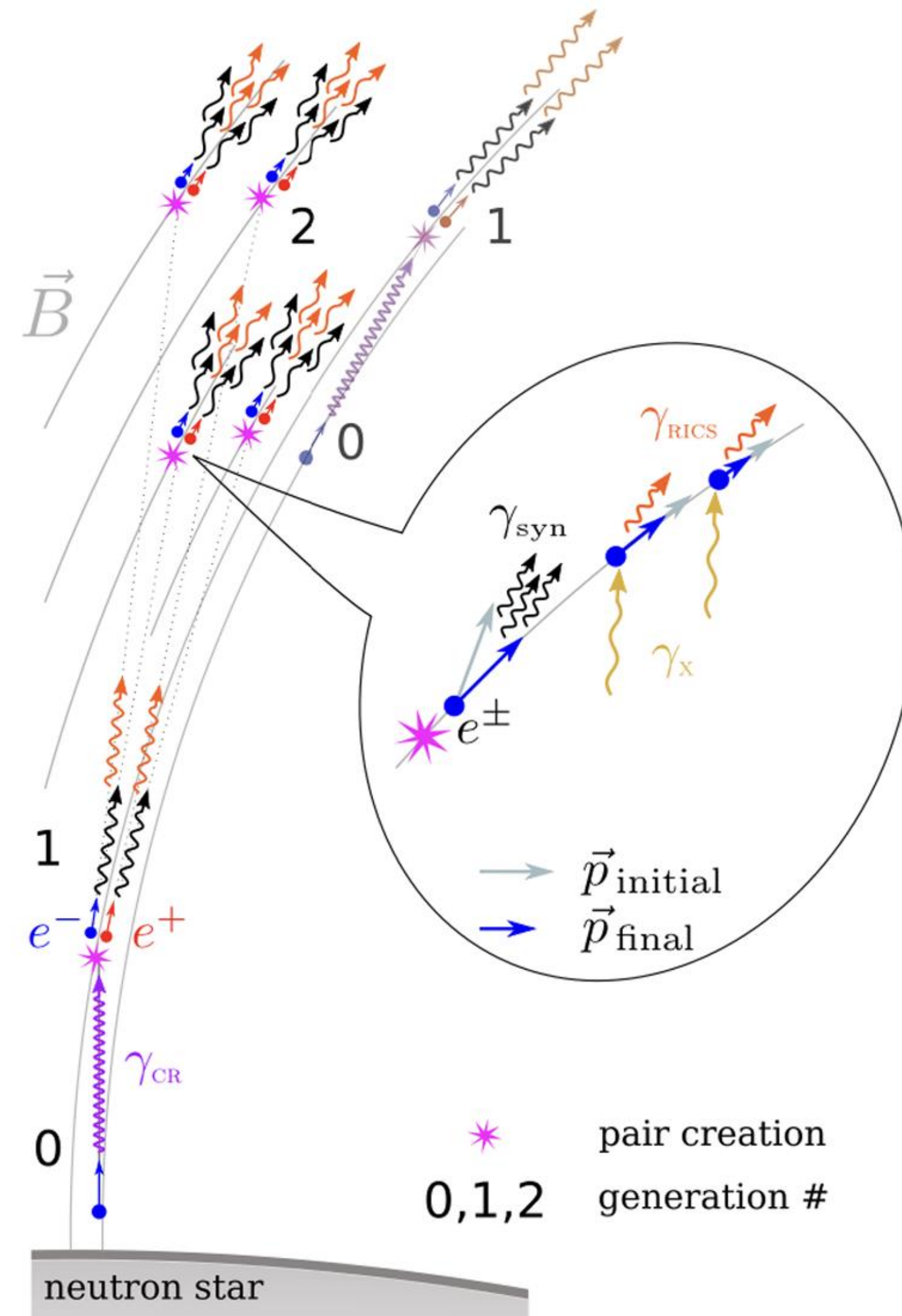
Charge density satisfies:

$$\nabla \cdot \mathbf{E} = 4\pi\rho$$

→

$$\rho_{\text{GJ}} = -\frac{\boldsymbol{\Omega} \cdot \mathbf{B}}{2\pi c} \frac{1}{1 - (\Omega r/c)^2 \sin^2 \theta}$$

$$n_{\text{GJ}} \equiv \rho_{\text{GJ}}/e \approx 7 \times 10^{10} \times \left(\frac{B_z}{10^{12} \text{G}}\right) \left(\frac{P}{1 \text{s}}\right)^{-1} \text{cm}^{-3}$$



Goldreich-Julian density (Goldreich & Julian 1969)

Amato 2024 arxiv.

Charged particles fill the pulsar surroundings → magnetized plasma → magnetosphere

Static magnetosphere:

$$q(\mathbf{E} + \mathbf{v} \times \mathbf{B}) = 0$$

Corotation condition:

$$\mathbf{E} + (\boldsymbol{\Omega} \times \mathbf{r}) \times \mathbf{B} = 0$$

Charge density satisfies:

$$\nabla \cdot \mathbf{E} = 4\pi\rho$$

→

$$\rho_{\text{GJ}} = -\frac{\boldsymbol{\Omega} \cdot \mathbf{B}}{2\pi c} \frac{1}{1 - (\Omega r/c)^2 \sin^2 \theta}$$

$$n_{\text{GJ}} \equiv \rho_{\text{GJ}}/e \approx 7 \times 10^{10} \times \left(\frac{B_z}{10^{12} \text{G}}\right) \left(\frac{P}{1 \text{s}}\right)^{-1} \text{cm}^{-3}$$

Goldreich-Julian density (Goldreich & Julian 1969)

Corotation: limited because

$$|\boldsymbol{\Omega} \times \mathbf{r}| < c$$

→ Light cylinder (LC):

$$R_{\text{LC}} = c/\Omega$$

Magnetic field lines

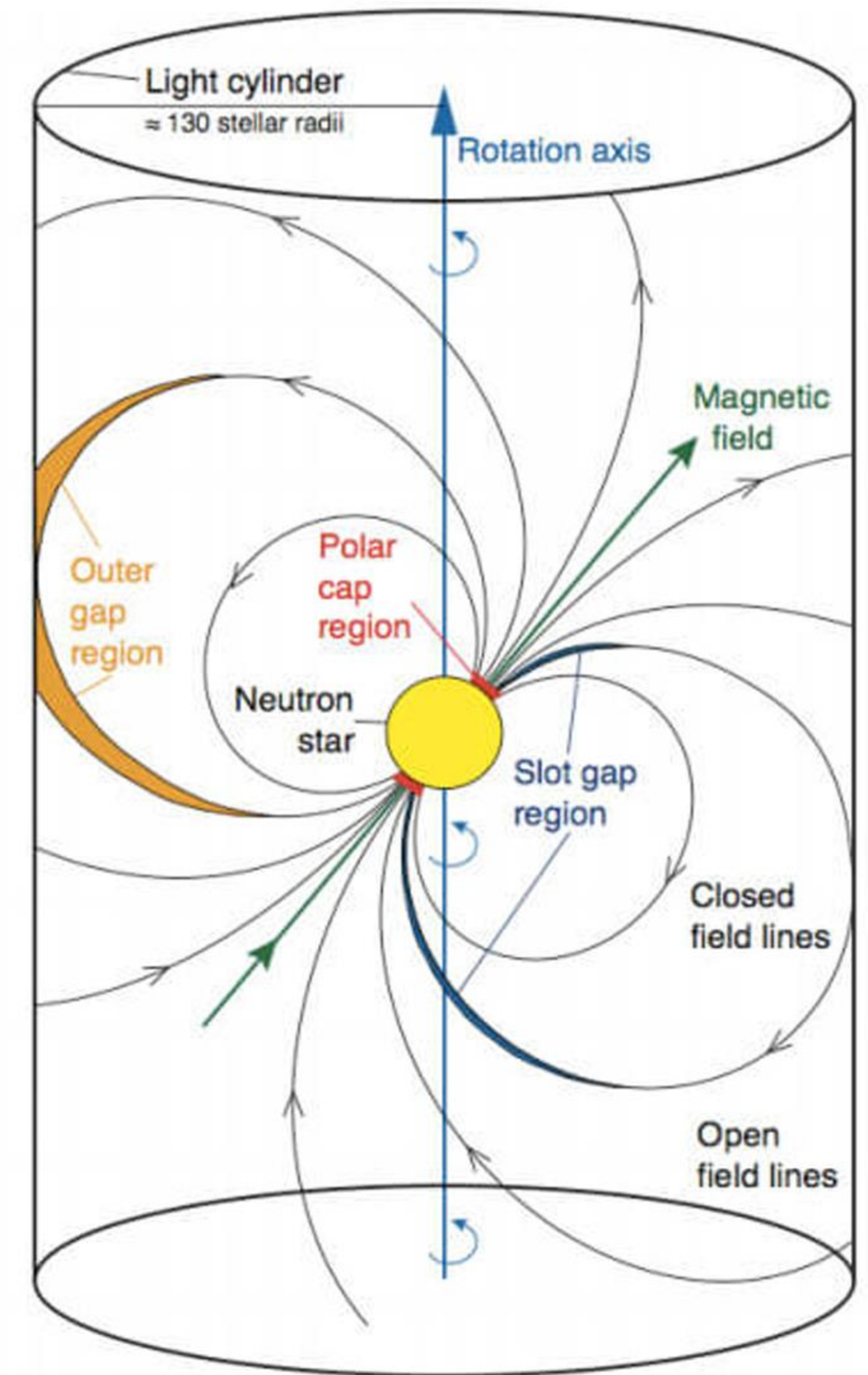
➤ Closed within LC:

**Closed field lines**

➤ Not closed within LC:

**Open field lines**

Feet of open field lines on pulsar surface: **Polar cap.**



Amato 2024 arxiv.

## (ii) Introduction to models

### (1) From Charge density driven to Current density driven:

From previous pages, we know when  $\rho \neq \rho_{GJ}$  at somewhere, the magnetosphere is no longer static (non-force-free, non-FFE).

But for open field lines region, the magnetosphere is naturally “non-static”:  
Open field lines **twist** at light cylinder  $\rightarrow$  always requires magnetospheric currents.

Use current density as indication for acceleration’s happening.

Introduce  $\alpha = j_{\parallel} / (\rho_{GJ} c)$

$0 < \alpha < 1$ : (mild relativistic  $\rho = \rho_{GJ}$  flow) or (ultra-relativistic  $\rho < \rho_{GJ}$  flow)  $\rightarrow$  no lack for charge

$\alpha > 1$ :  $|\rho| > |\rho_{GJ}|$  flow  $\rightarrow$  charge starvation  $\rightarrow$  parallel electric field arises

$\alpha < 0$ : net charge decrease  $\rightarrow$  charge starvation  $\rightarrow$  parallel electric field arises

## (2) Ruderman-Sutherland (RS) model v.s. Space-Charge-Limited-Flow (SCLF) model:

RS model (Ruderman & Sutherland 1975): no supplement of plasma from pulsar surface.  
(With isolated “sparks” → can explain subpulse drifting)

SCLF mode (Arons & Scharlemann 1979...): ions & electrons supplied by pulsar surface/atmosphere.

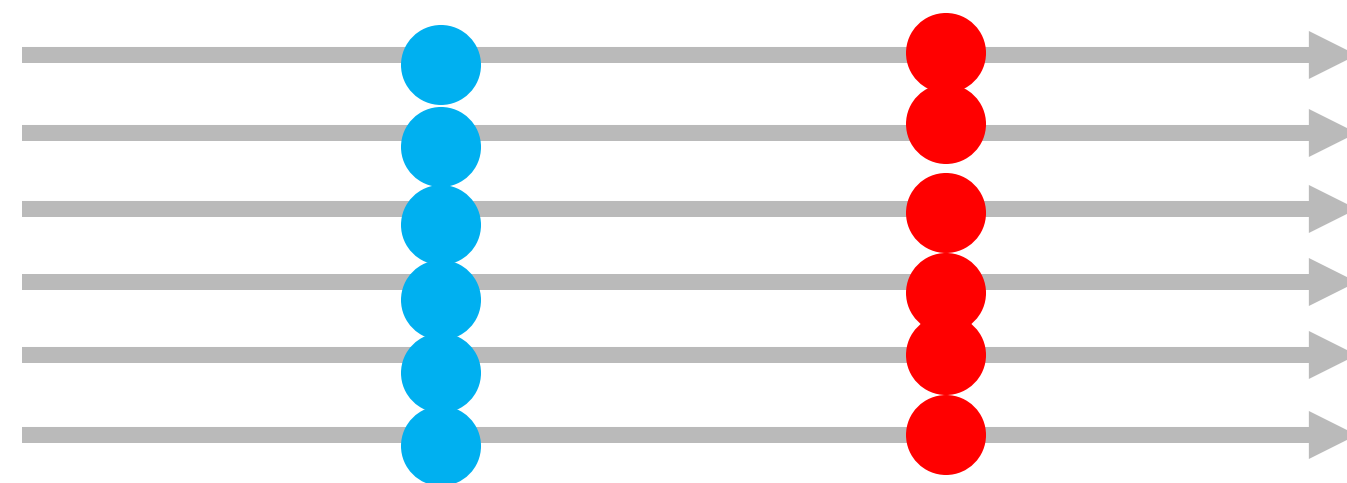
(Different in binding energy at pulsar surface)

## (3) Coherent radio emission mechanism:

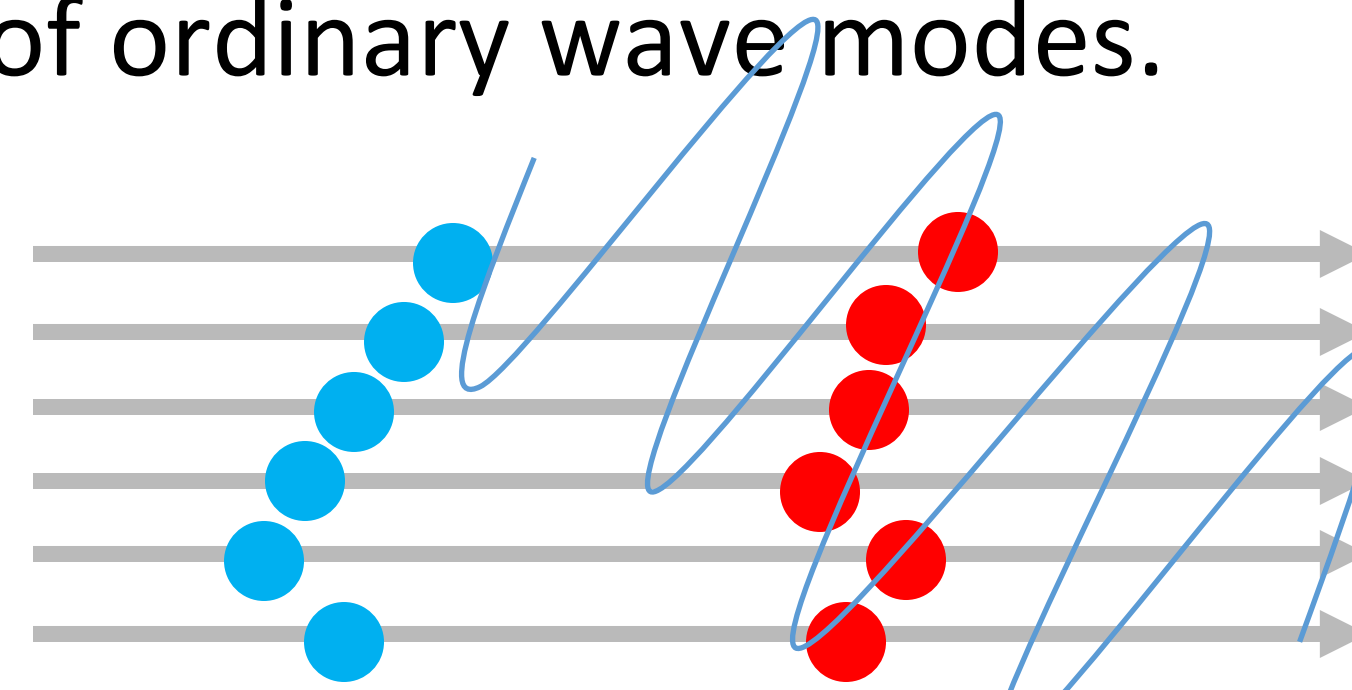
Simulation by Philippov, Timokhin & Spitkovsky 2020:

Spatial inhomogeneous discharge causes excitation of ordinary wave modes.

This paper:  
2D & 3D simulations  
On discharge processes



Homogeneous: Oscillation // Magnetic field



Inhomogeneous

# II. Simulation setups

## (1) EM dynamics

Unperturbed (Force-Free, FFE):  $\mathbf{B}_{\text{FFE}} = \mathbf{B}_0 + \mathbf{B}_\varphi$ ,  $\mathbf{E}_{\text{FFE}} = -\boldsymbol{\Omega} \times \mathbf{r} \times \mathbf{B}_0/c$   $\rho_{\text{GJ}} = \nabla \cdot \mathbf{E}_{\text{FFE}}/4\pi$

Corrections:  $\frac{\partial}{\partial t} \delta \mathbf{E} = c \nabla \times \delta \mathbf{B} - 4\pi(\mathbf{j} - \mathbf{j}_{\text{mag}})$ ,  
 $\frac{\partial}{\partial t} \delta \mathbf{B} = -c \nabla \times \delta \mathbf{E}$ .  $\nabla \cdot \delta \mathbf{E} = 4\pi(\rho - \rho_{\text{GJ}})$

Polar cap:  $R_{\text{PC}} = R_\star \sqrt{R_\star/R_{\text{LC}}}$   $R_{\text{LC}} = cP/2\pi$

Two stationary solutions:

- (i)  $\delta E = \delta B = 0$ , fully force free,  $\dot{j} = \dot{j}_{\text{mag}}$   $\leftarrow$  Abundant plasma everywhere
- (ii)  $j = 0$ ,  $\delta B = -B_\varphi$ , no magnetic field twist  $\leftarrow$  No plasma loading



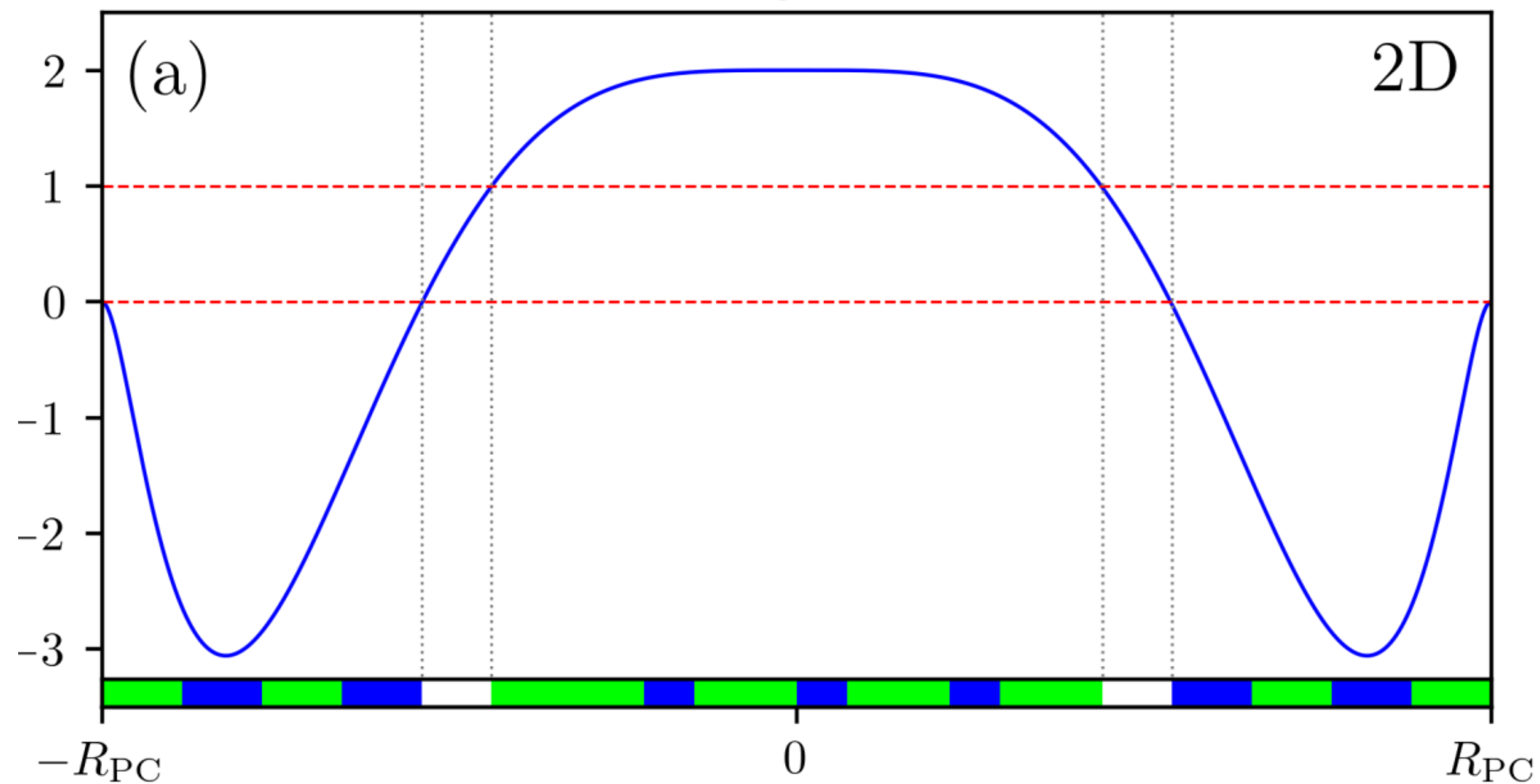
## (2) Magnetospheric current distribution: follow Gralla et al. 2016, 2017

2D:  $j_{\text{mag}}^{2\text{D}}(x) = 2 - C_1 x^4 + C_2 x^6 + C_3 x^{40}$

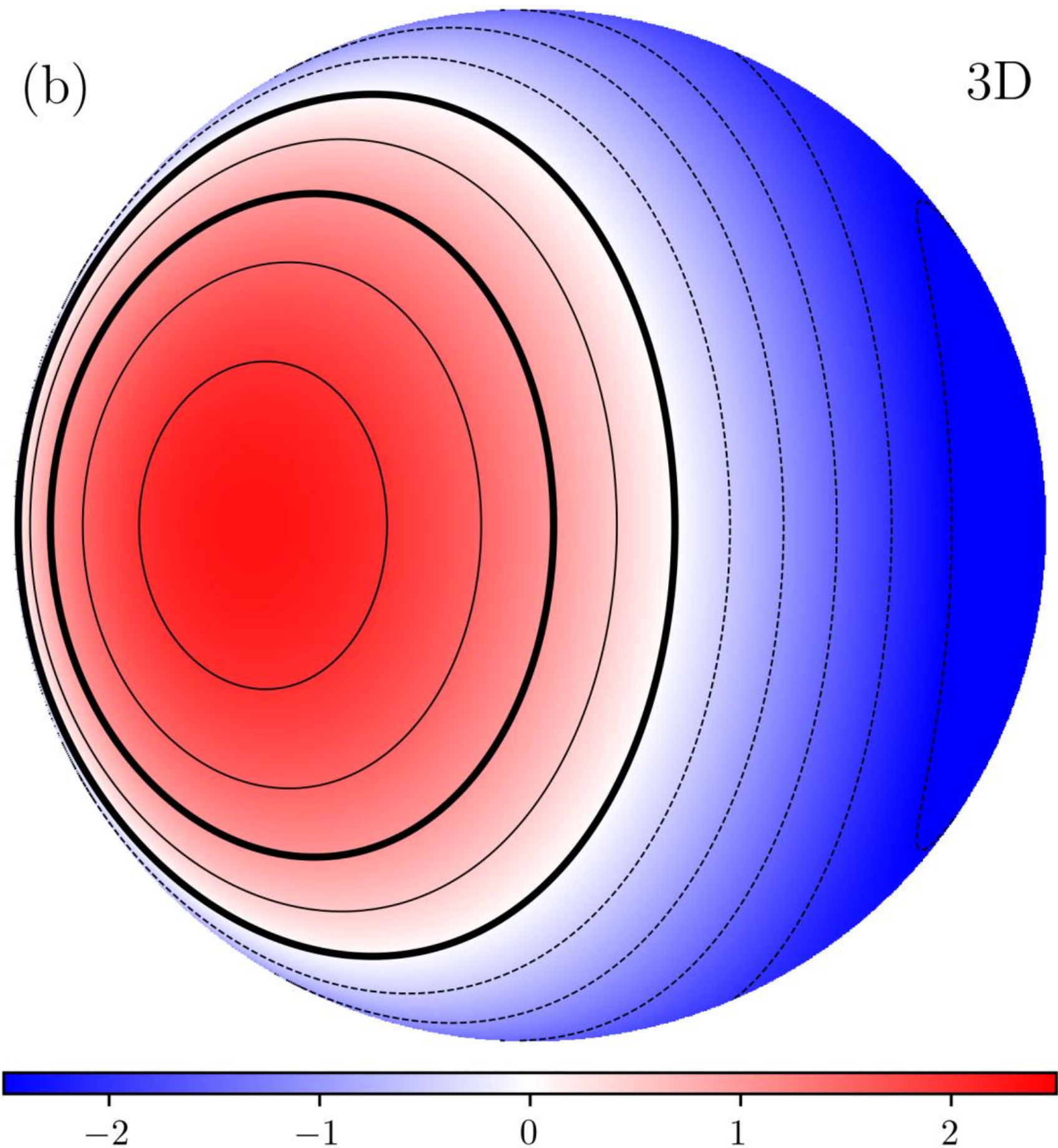
$$\int_0^{R_{\text{PC}}} j_{\text{mag}}^{2\text{D}} dx = 0, \quad j_{\text{mag}}^{2\text{D}}(1) = 0, \quad \left. \frac{d}{dx} j_{\text{mag}}^{2\text{D}} \right|_{x=1} = 0.$$

$$x = r_{\perp} / R_{\text{PC}}$$

$$j_{\text{mag}} / j_{\text{GJ}}$$



3D:  $\frac{j_{\text{mag}}^{3\text{D}}}{\rho_{\text{GJ}} c}(\theta, \phi) \approx \frac{1}{(1 - \Omega_Z / \Omega)} [J_0(\arcsin(\theta / \sqrt{\alpha_0})) - J_1(\arcsin(\theta / \sqrt{\alpha_0})) \tan i \cos \phi].$



(3) QED pair creation  $\rightarrow$  leads to large multiplicity  $\mathcal{M} = n_{\pm}/n_{\text{GJ}} \gg 1$

Emission in polar cap: synchrotron curvature radiation.

$$\frac{dN_{\text{ph}}}{dt d\varepsilon} = \frac{1}{\sqrt{3}\pi} \frac{e^2}{\hbar^2 c} \frac{1}{\gamma_b^2} \int_{\frac{\varepsilon}{\varepsilon_{\text{ph}}^*}}^{\infty} K_{5/3}(x) dx, \quad \varepsilon_{\text{ph}}^* = \frac{3}{2} \hbar \frac{c}{\rho_c} \gamma_b^3.$$

Cross section for pair creation:

$$\frac{d\sigma}{dz} = 0.23 \frac{B}{B_q} \sin \psi \frac{\alpha_F}{\lambda_c} \exp\left(-\frac{8}{3\chi}\right) \Theta(\tilde{\varepsilon}_{\text{ph}} \sin \psi - 2), \quad \chi = (B/B_q) \tilde{\varepsilon}_{\text{ph}} \sin \psi \quad \tilde{\varepsilon}_{\text{ph}} = \varepsilon_{\text{ph}}/m_e c^2$$

$$B_q = m_e^2 c^3 / e \hbar \approx 4.41 \times 10^{13} \text{G}$$

Secondary particles' velocity:

$$u_{\parallel} = \frac{|\cos \psi_a| (\tilde{\varepsilon}_{\text{ph}}^2 - 4)^{1/2}}{(\tilde{\varepsilon}_{\text{ph}}^2 \sin^2 \psi_a + 4 \cos^2 \psi_a)^{1/2}} \sim \frac{1}{\sin \psi_a} \sim 10^2 - 10^3,$$

Pair creation & emission energy scales described in 3 gamma parameters:

$$\gamma_{\text{PC}} = 0.5 (R_{\text{PC}}/d_e^{\text{GJ}})^2 \quad eE_{\text{PC}} = (2/3) e^2 \gamma_{\text{rad}}^4 / \rho_c^2 \quad (3/2) \hbar (c/\rho_c) \gamma_{\text{emit}}^3 = m_e c^2$$

$$d_e^{\text{GJ}} = c / \sqrt{4\pi |\rho_{\text{GJ}} e| / m_e} \quad \tilde{\varepsilon}_{\text{ph}} = (\gamma/\gamma_{\text{emit}})^3$$

Generally,  $\gamma_{\text{PC}} \gg \gamma_{\text{rad}} \gg \gamma_{\text{emit}}$ .

## (4) Atmosphere

SCLF model: thin electron-ion atmosphere → reservoir of charged particles.

≈ A hot plasma layer at simulation boundary.  $n = n_{\text{peak}} \exp(-z/h)$

(This  $T$  is about  $2.5 \times 10^4$  K.)

$$h = kT / (m_e g) \approx 10 d_e^{\text{GJ}}$$

$$n_{\text{peak}} \approx 10 n_{\text{GJ}}$$

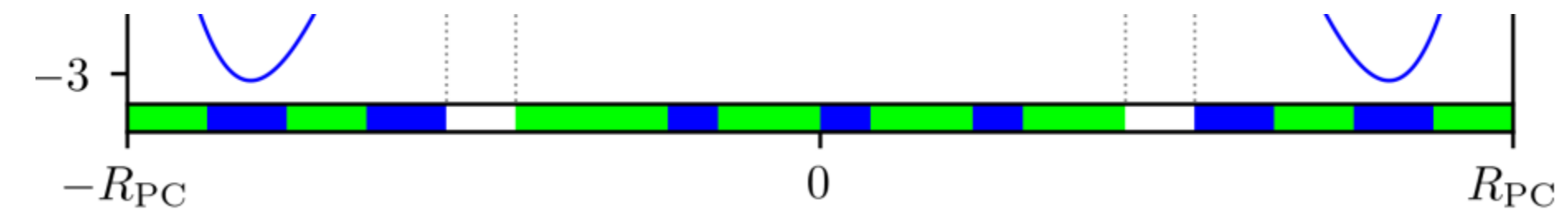
RS model: no atmosphere.

## (5) Initial plasma state

Multiplicity ~ a few.  $j = j_{\text{mag}}$   $\delta \mathbf{E} = 0$   $\rho_{\text{GJ}} = \rho_{\text{GJ}}^0 (1 + 0.8z/L_z)$

Initial inhomogeneity: divide polar cap into different patches.

stop injecting initial plasma at different times on neighboring patches.



## (6) Numerical details

Tristan-v2: multi-species radiative PIC code (Hakobyan et al. 2024).

Initial magnetic field: uniform. Curvature of field lines: prescribed. Multiplicity < 50...

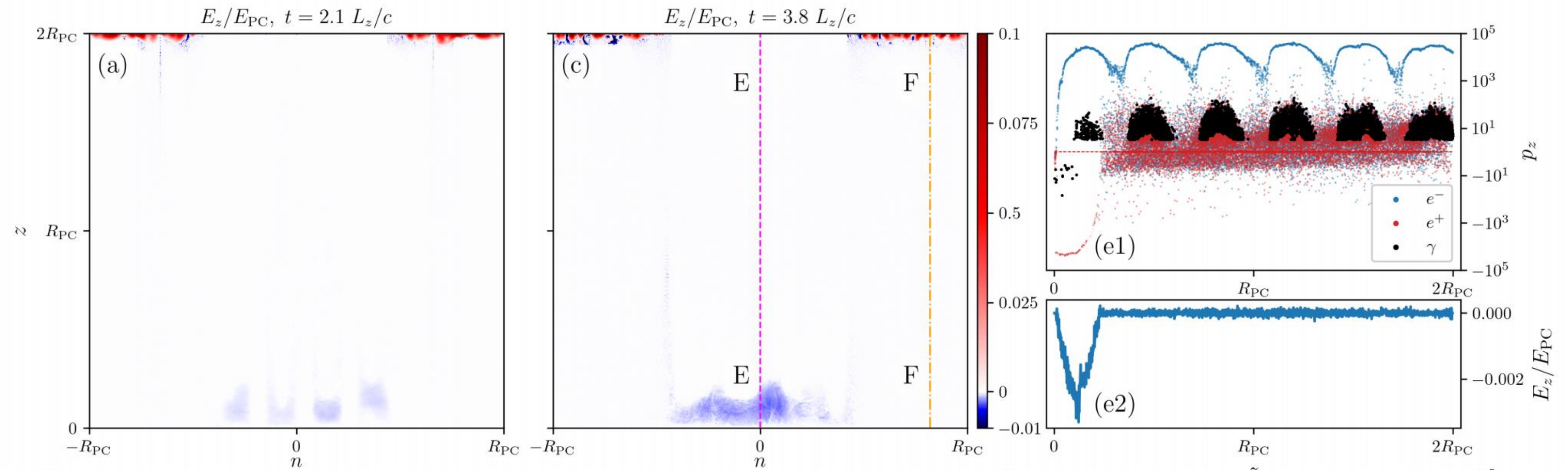
# III. Results

## (1) SCLF

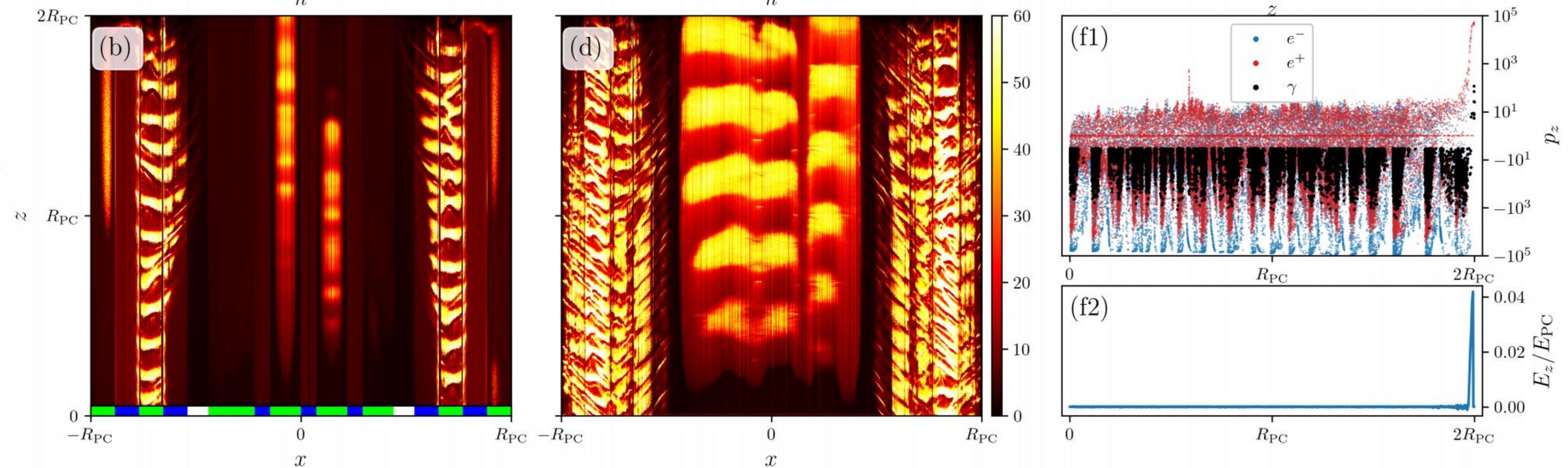
### (1.1) Small gap & Constant field lines' curvature

Dipolar field with multipolar components?

$E_{//}$  field:



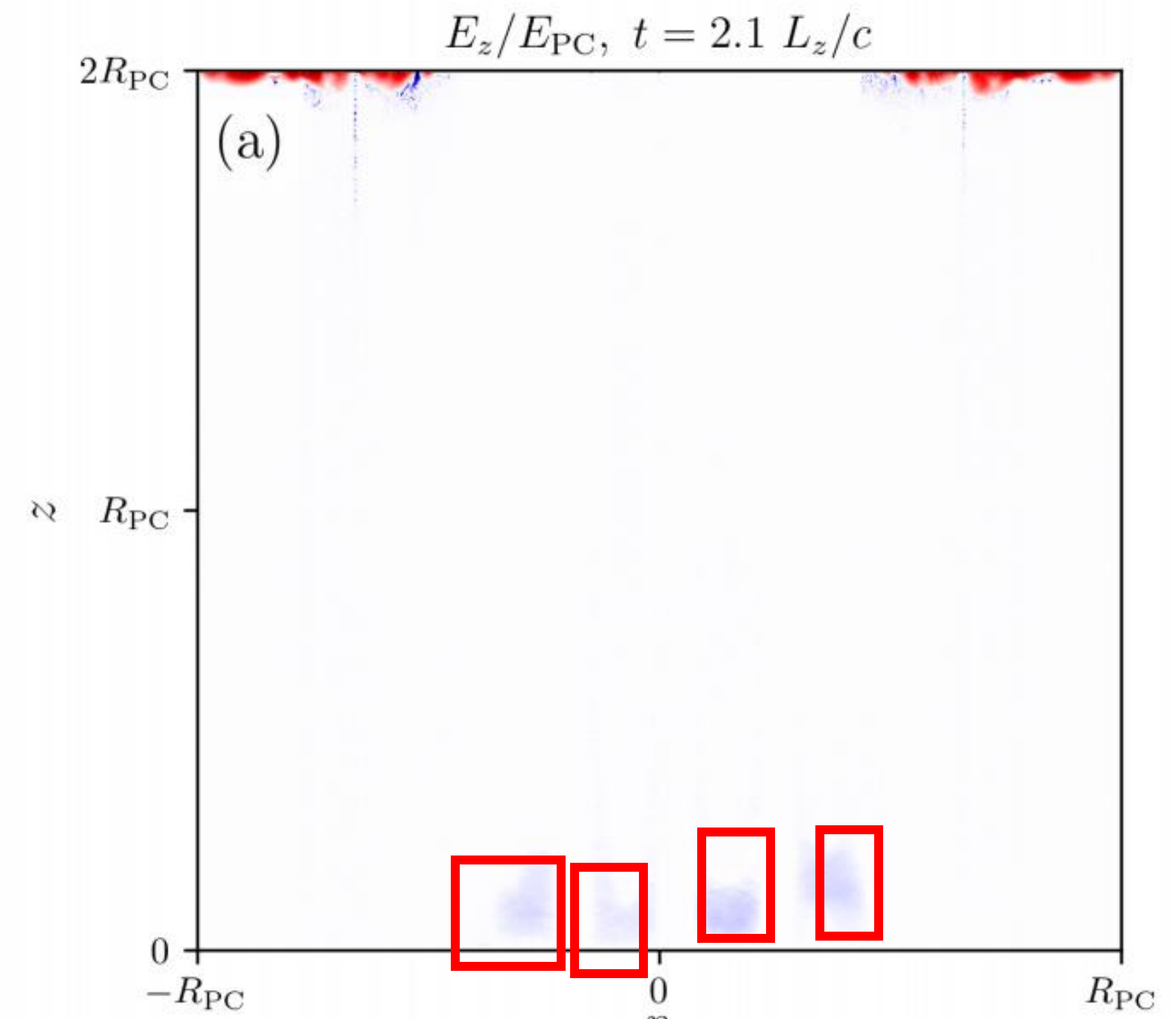
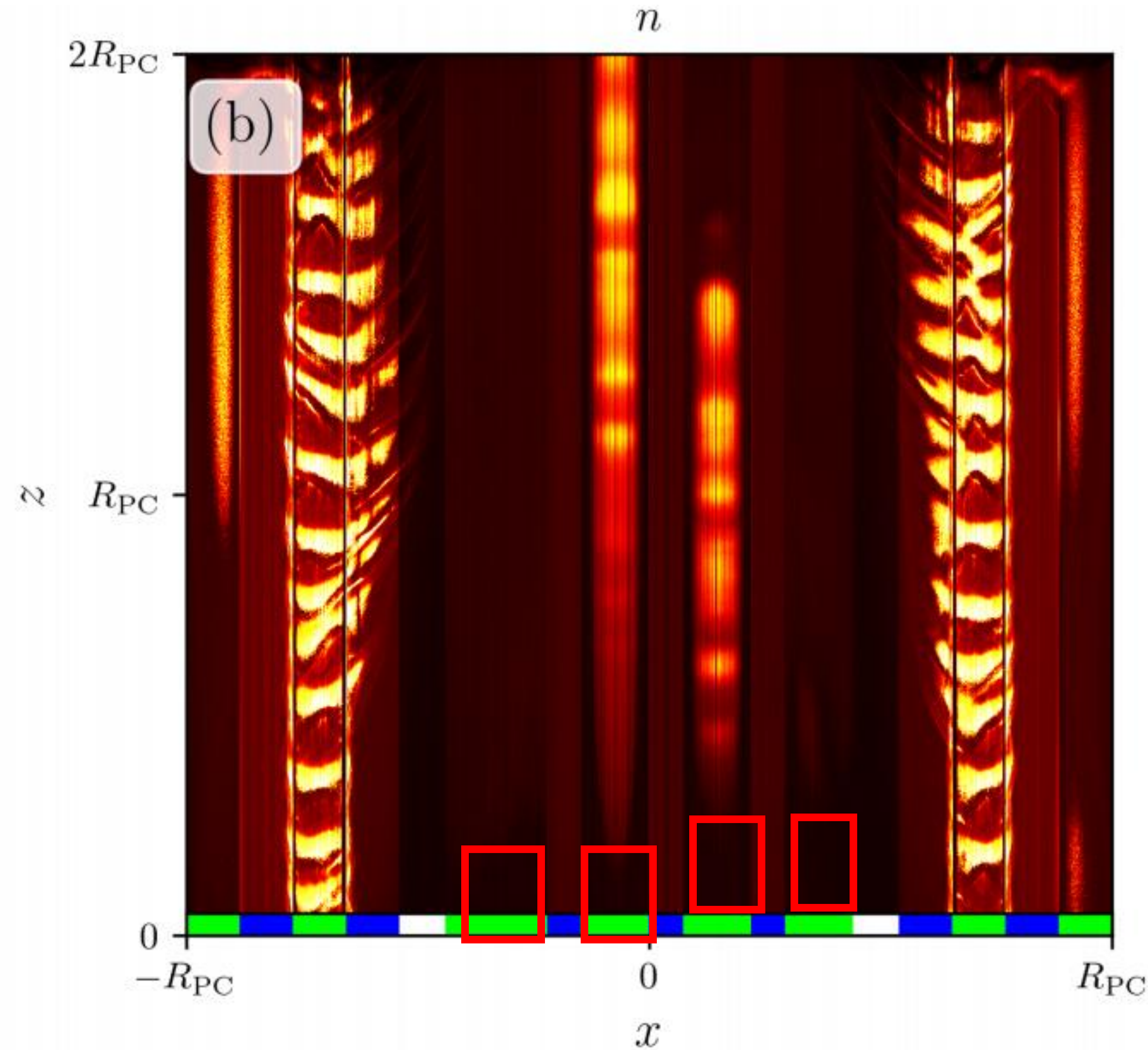
Particle number density:



Super-GJ region ( $j/j_{GJ} > 1$ ): gap close to surface.

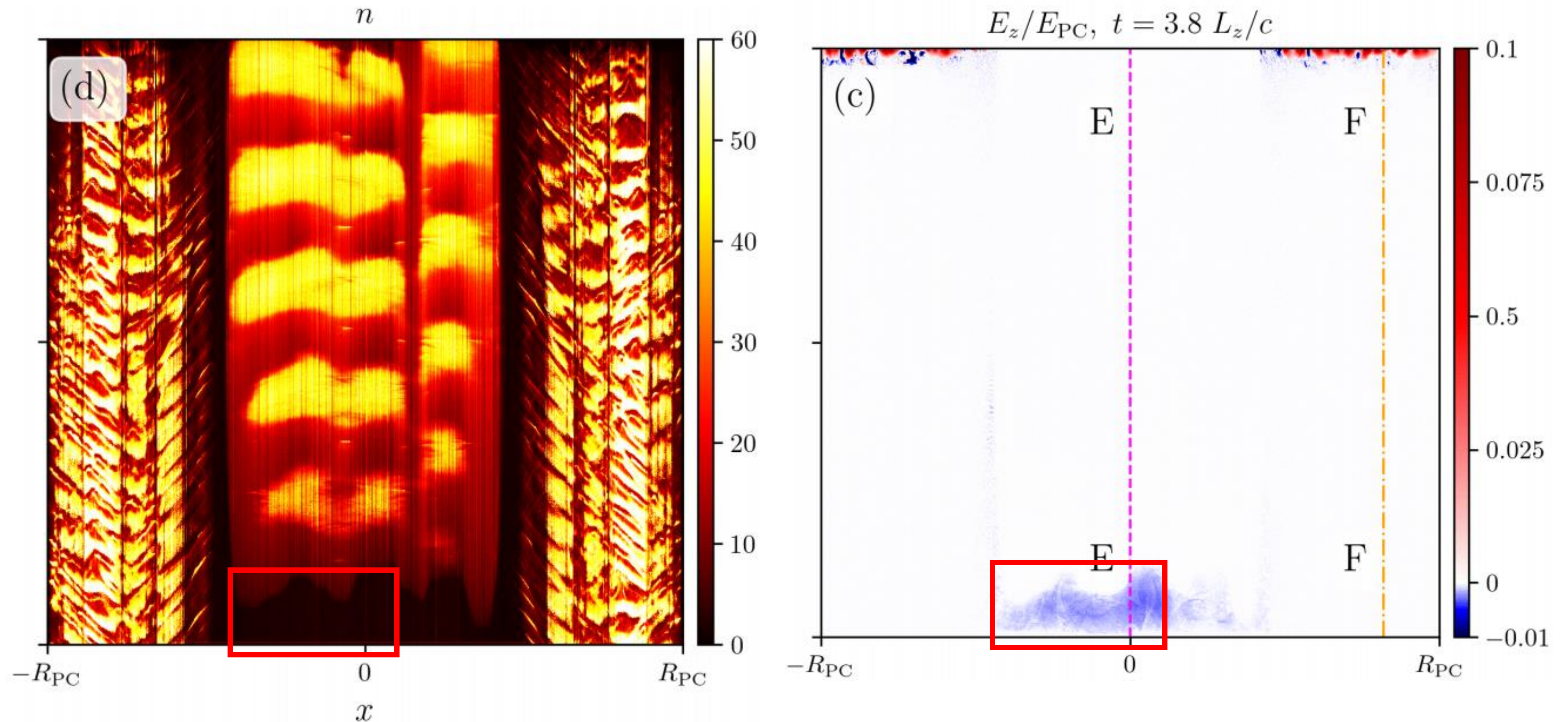
Early time: due to initial inhomogeneity sets, some patches have cleared plasma region, while some have not.

→ → Gaps are also in patches. And they are quasi-stationary.



Super-GJ region ( $j/j_{\text{GJ}} > 1$ ): gap close to surface.

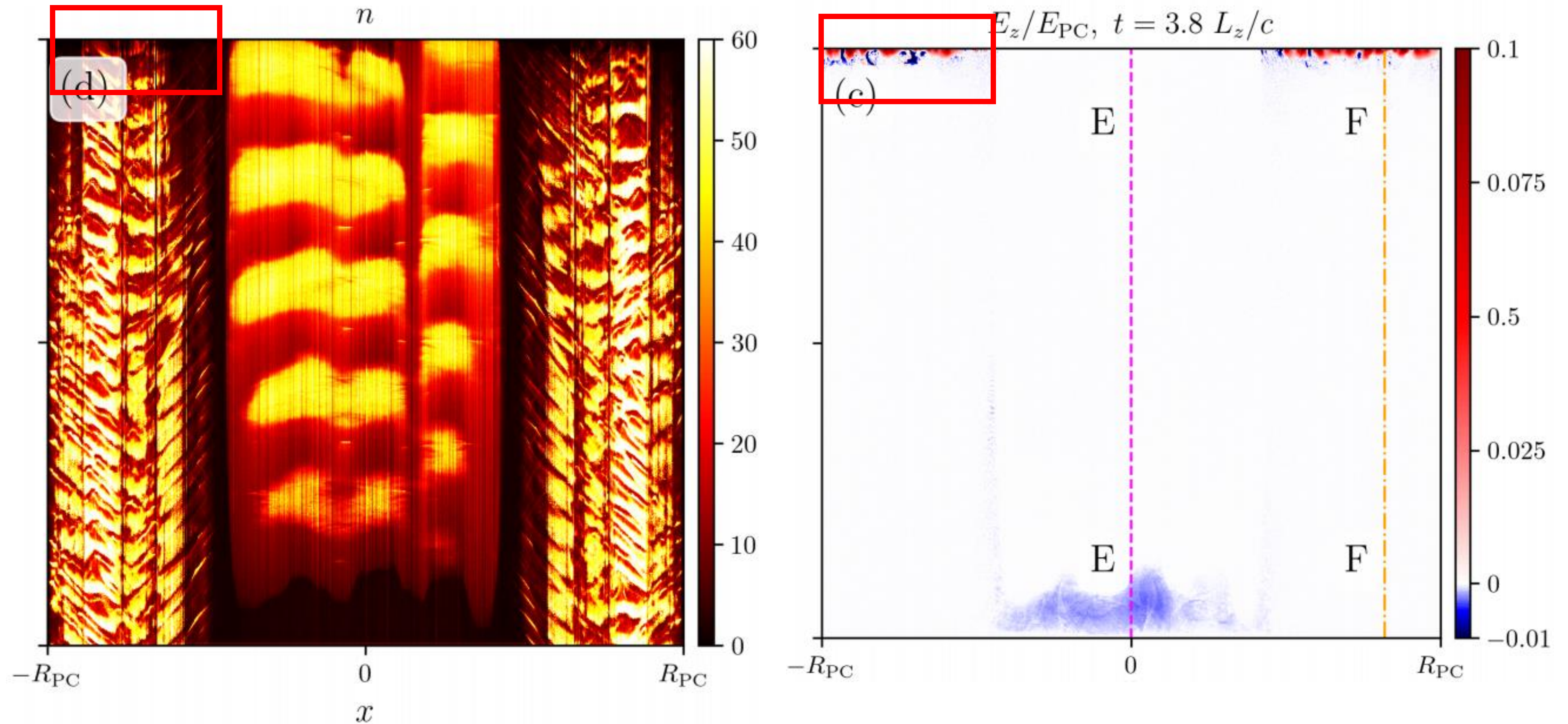
Late time: more patches clear plasma  $\rightarrow$  gaps are connected to **larger pieces**.



Cyclic screening happens  $\rightarrow$  Discharges are intermittent.

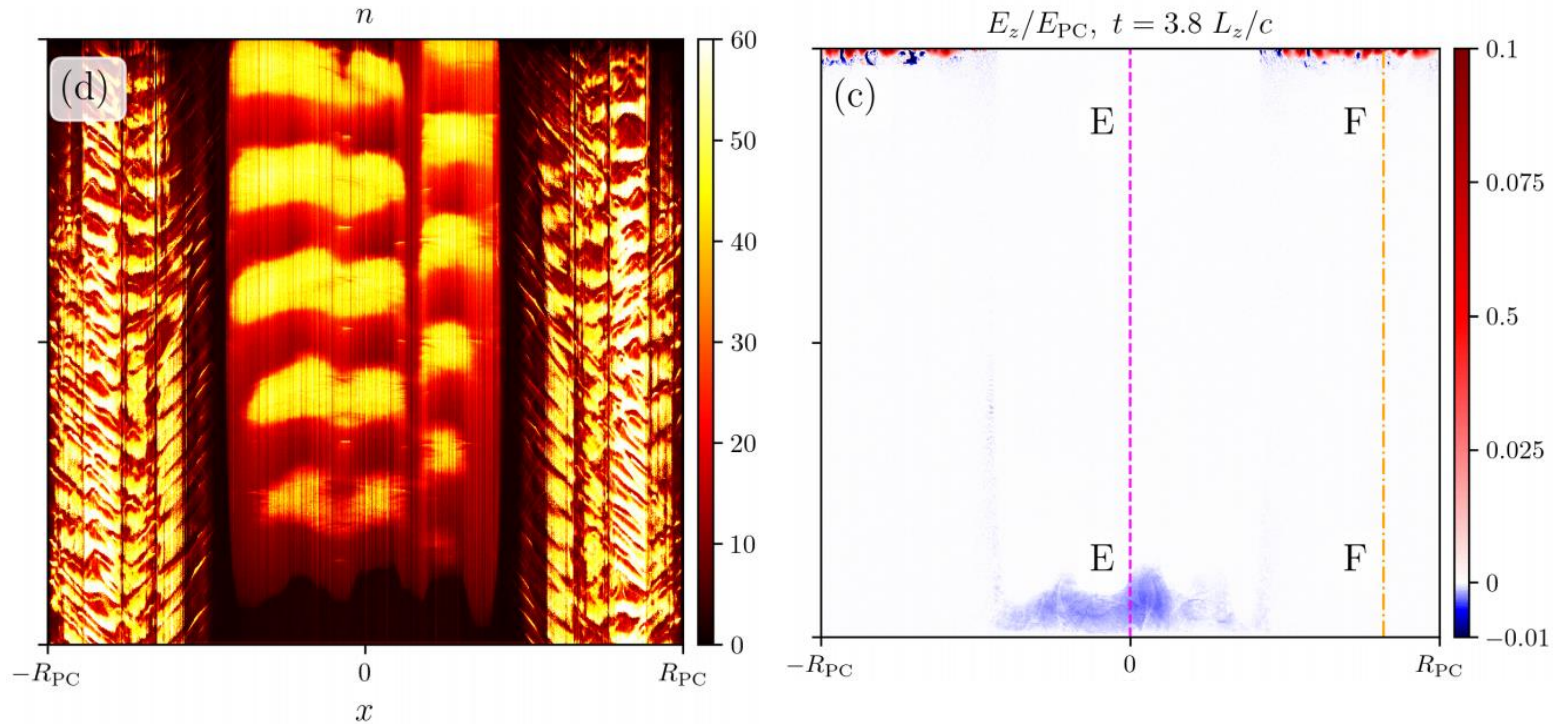
Return current region ( $j/j_{GJ} < 0$ ): higher gap.

Larger difference in motions of positrons & electrons  $\rightarrow$  stronger electric field  $\rightarrow$  smaller gaps



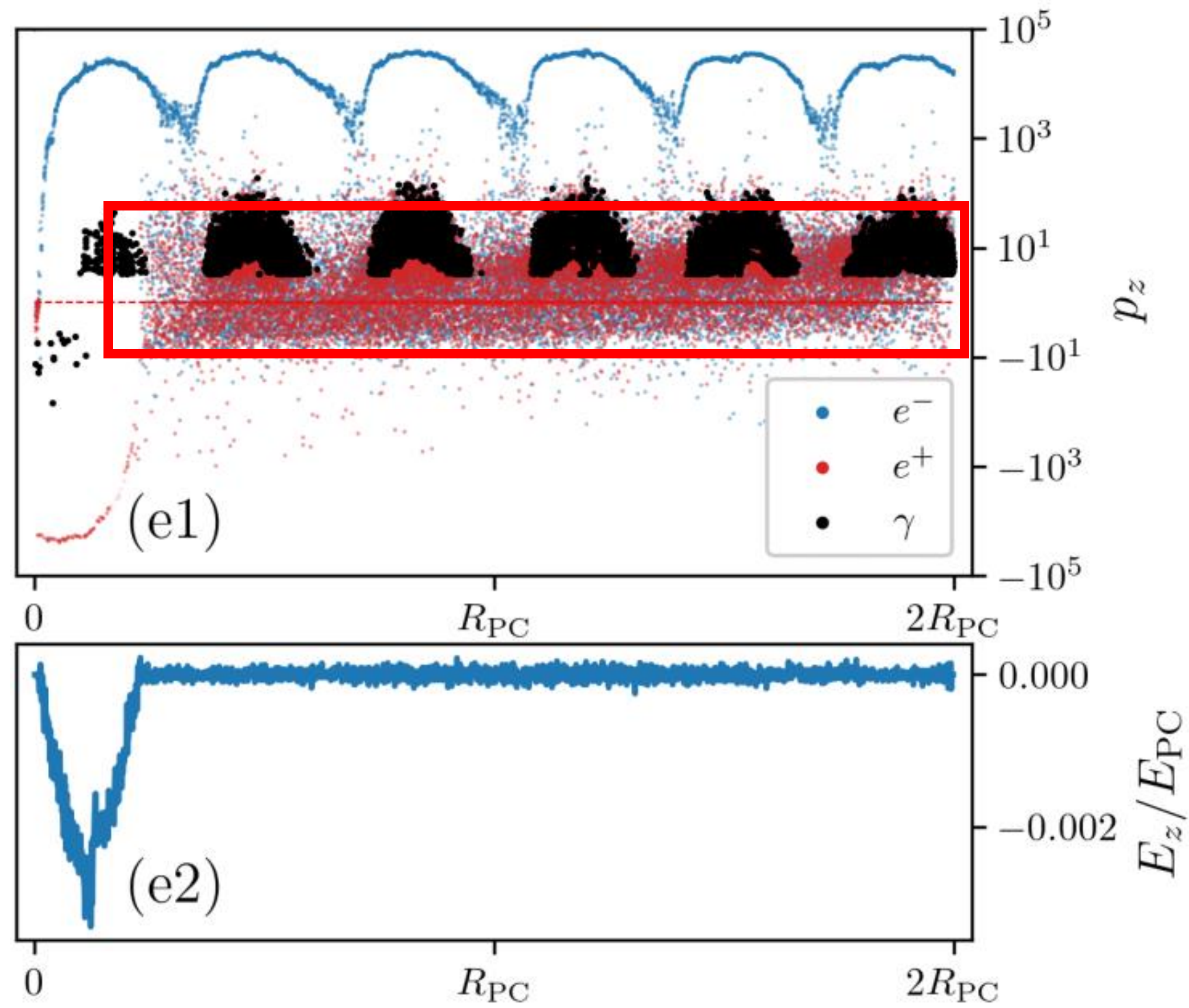
Cyclic screening happens  $\rightarrow$  Discharges are intermittent.

Transverse coherence scale of gaps  $< 2 * l_{\text{gap}}$   $\rightarrow$  Desynchronization of discharges.

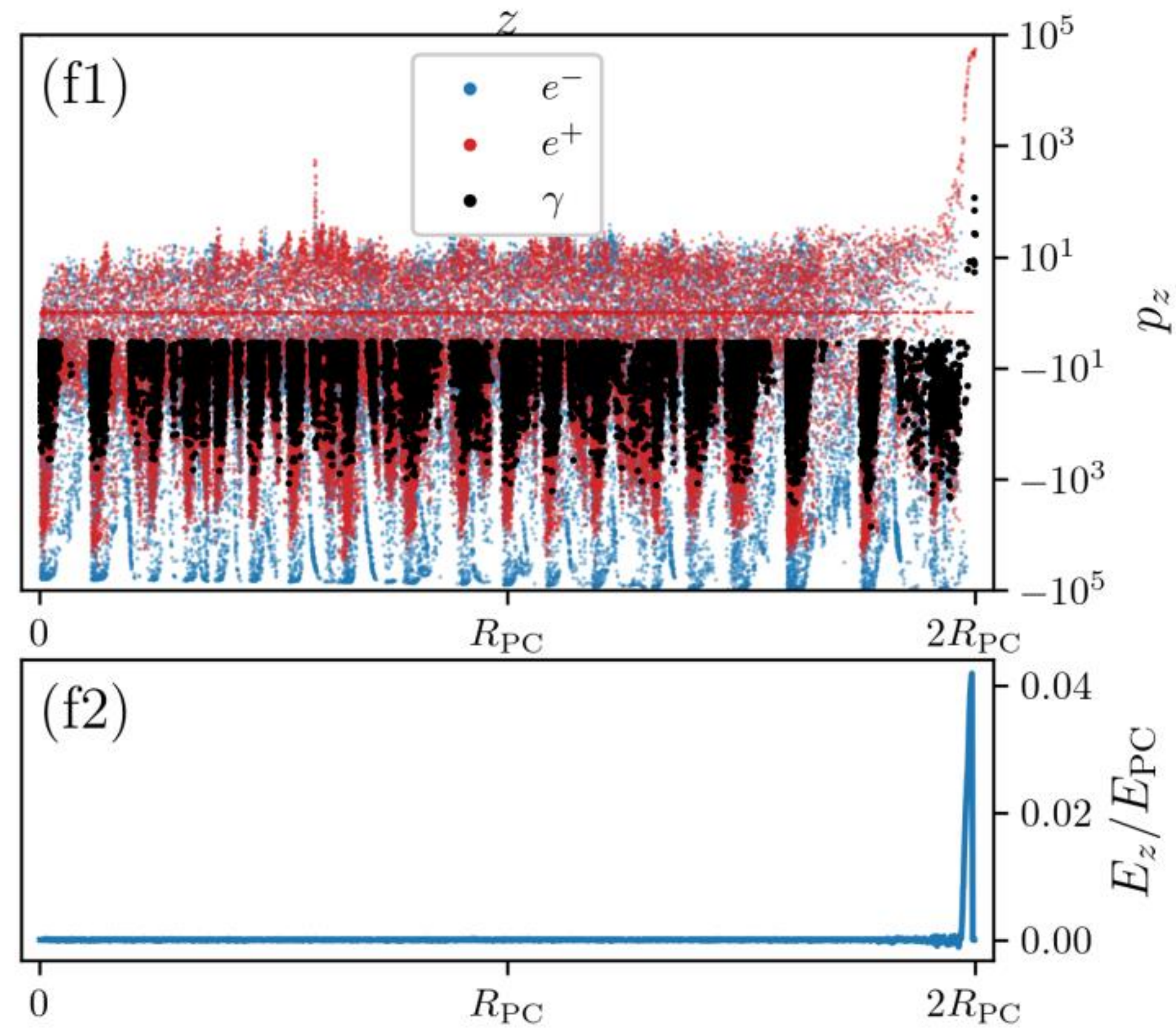




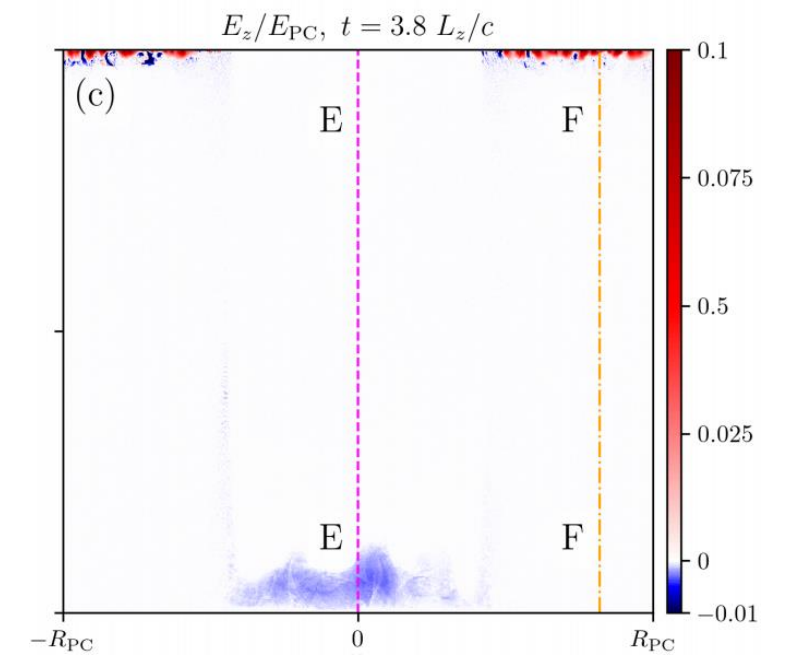
Difference in particle momentums and electric field for two kinds of gaps:



$j/j_{GJ} > 1$



$j/j_{GJ} < 0$

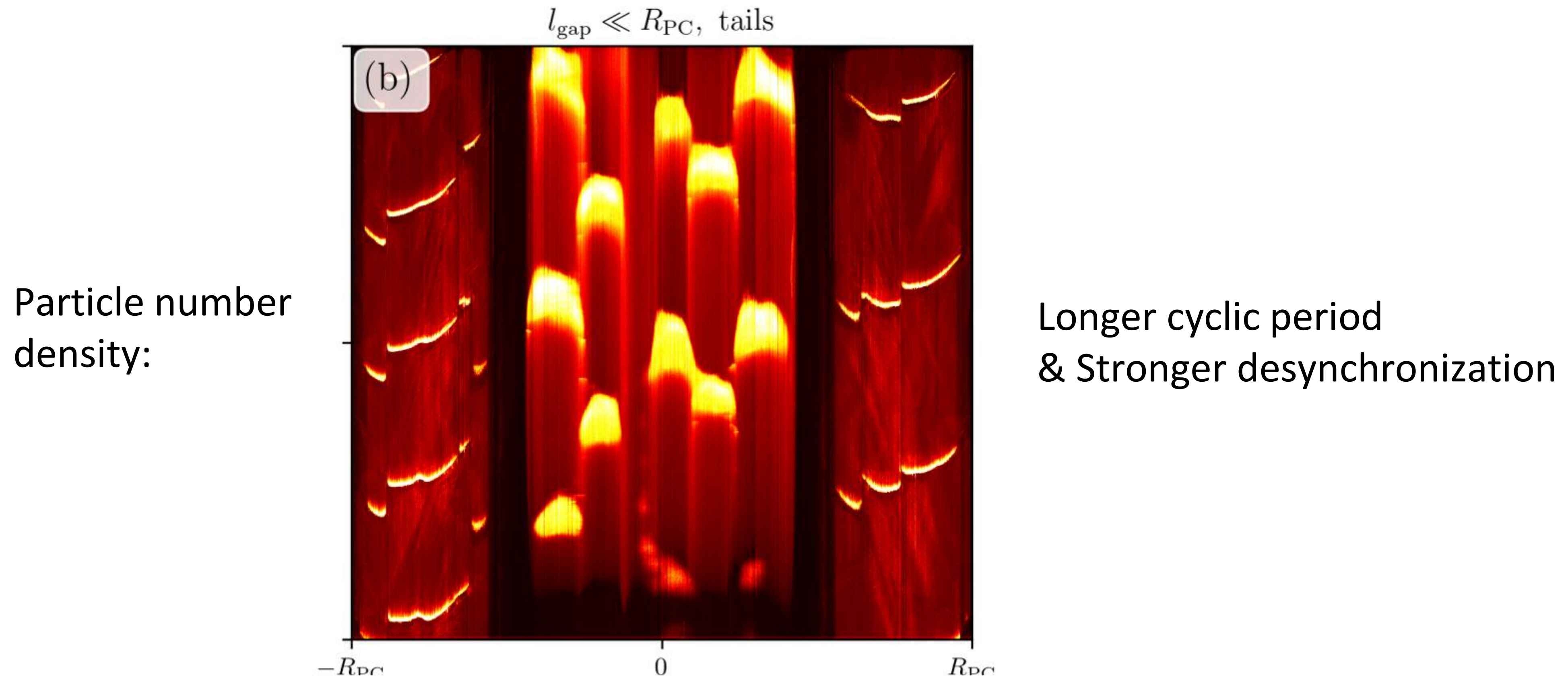


## (1.2) Small gap & Strong Desynchronization (more plasma)

Discharge cyclic period too short → reverse bombardment too strong → surface too hot  
→ can't fit X-ray observation

Actually caused by too low plasma density in simulation.

→ To fix it, the authors inject **additional** extended tails behind escaping clouds of secondary plasma

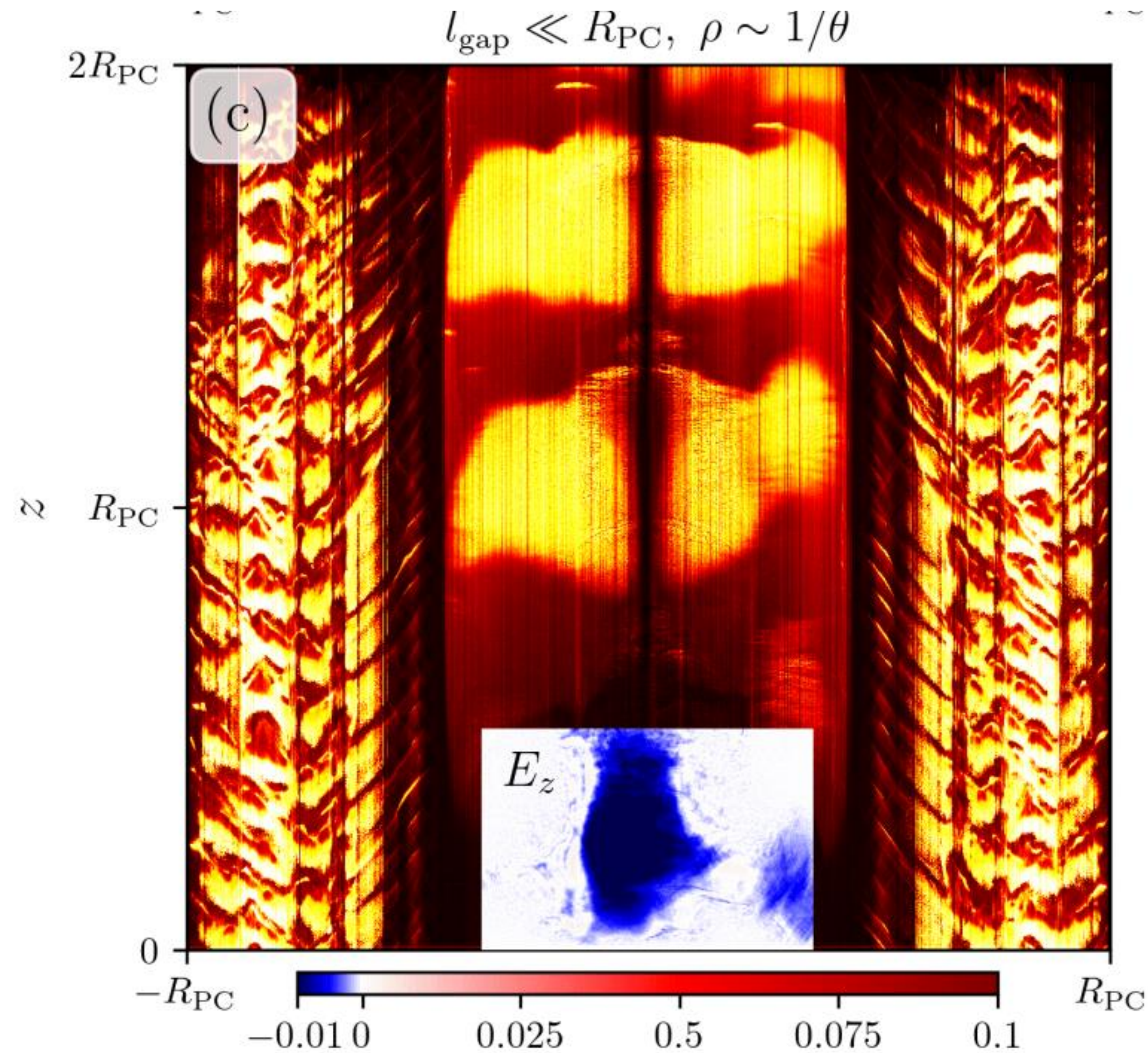


### (1.3) Small gap & Quasi dipolar field

$$\rho_c = \rho_{c,0}(R_{PC}/x)$$

When  $x \rightarrow 0$ ,  $\rho \rightarrow \infty \rightarrow$  discharge is absent at the center.

Particle number density:



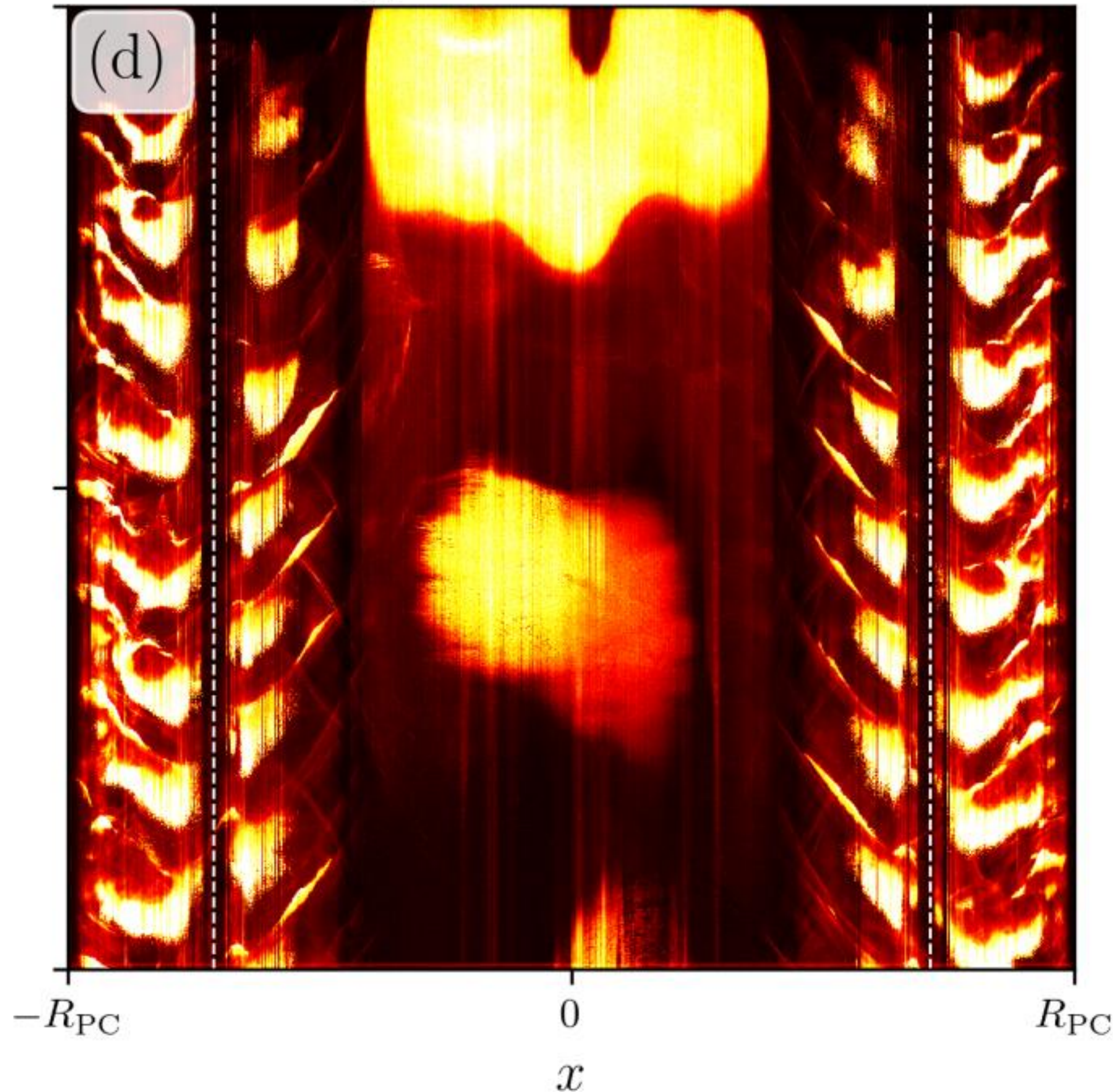
Larger gap.

Front of screening inclined  
 $\rightarrow$  benefit emission  
(See page 7)

# (1.4) Large gap ← less energetic pulsars

Smaller electric field for acceleration.

$$l_{\text{gap}} < R_{\text{PC}}, \rho = \text{const}$$



Particle number density:

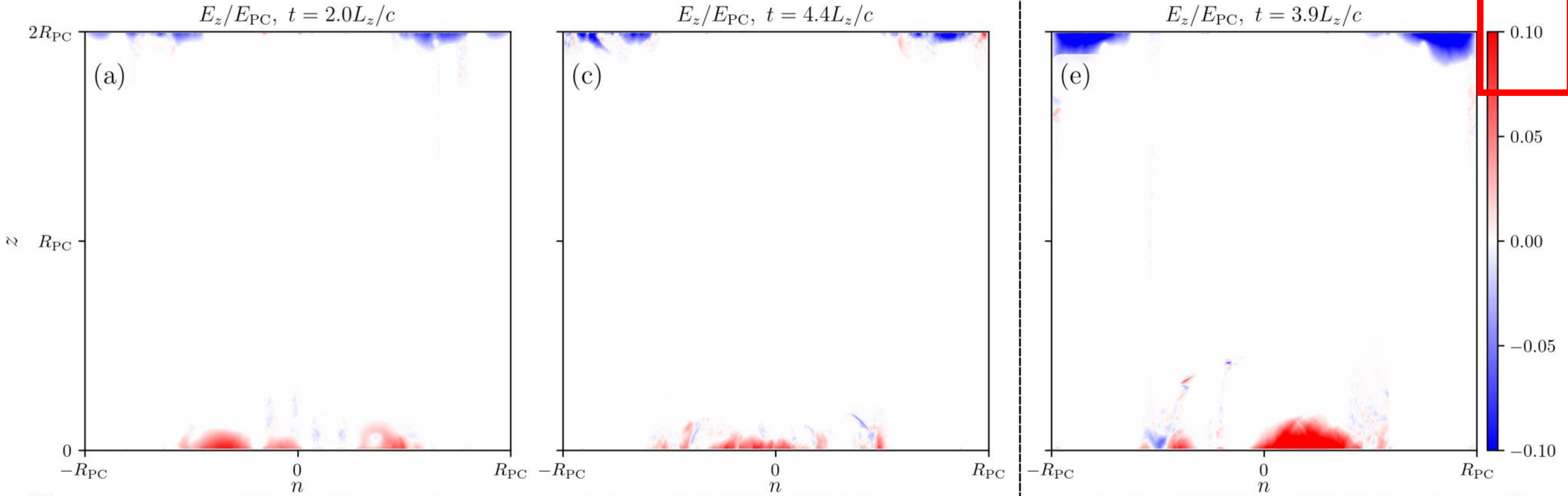
Longer cyclic period.

(2) RS model: generally similar to SCLF, but with larger electric field for  $j/j_{GJ} > 1$

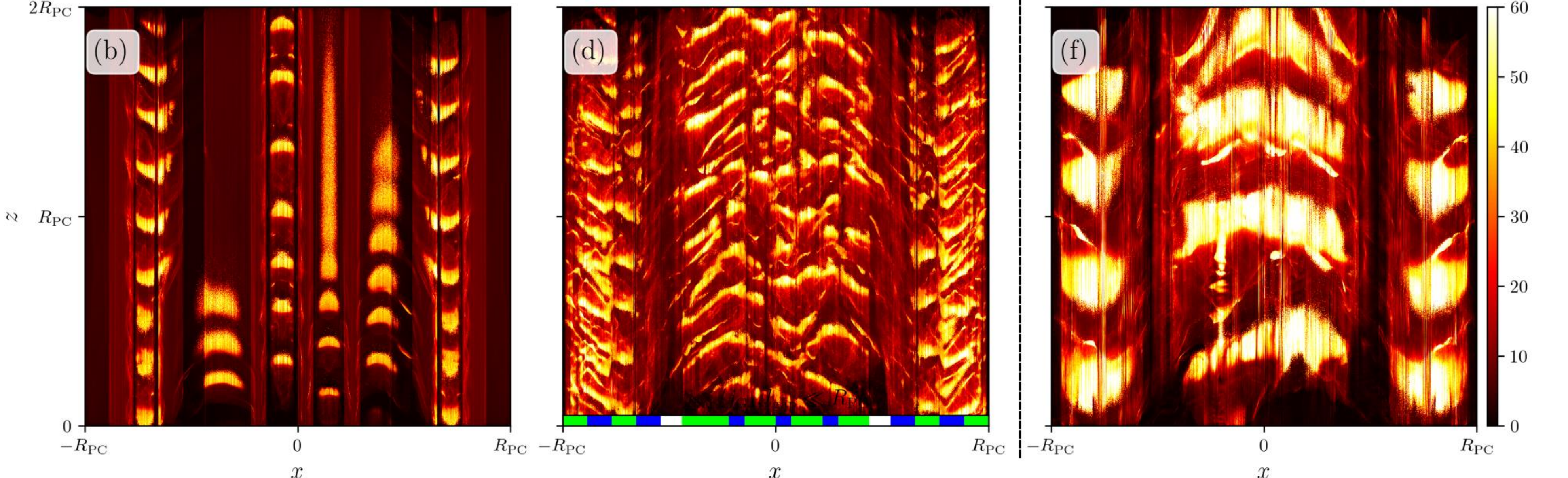
$l_{\text{gap}} \ll R_{\text{PC}}$

$l_{\text{gap}} < R_{\text{PC}}$

$E_{//}$  field:



Particle number density:

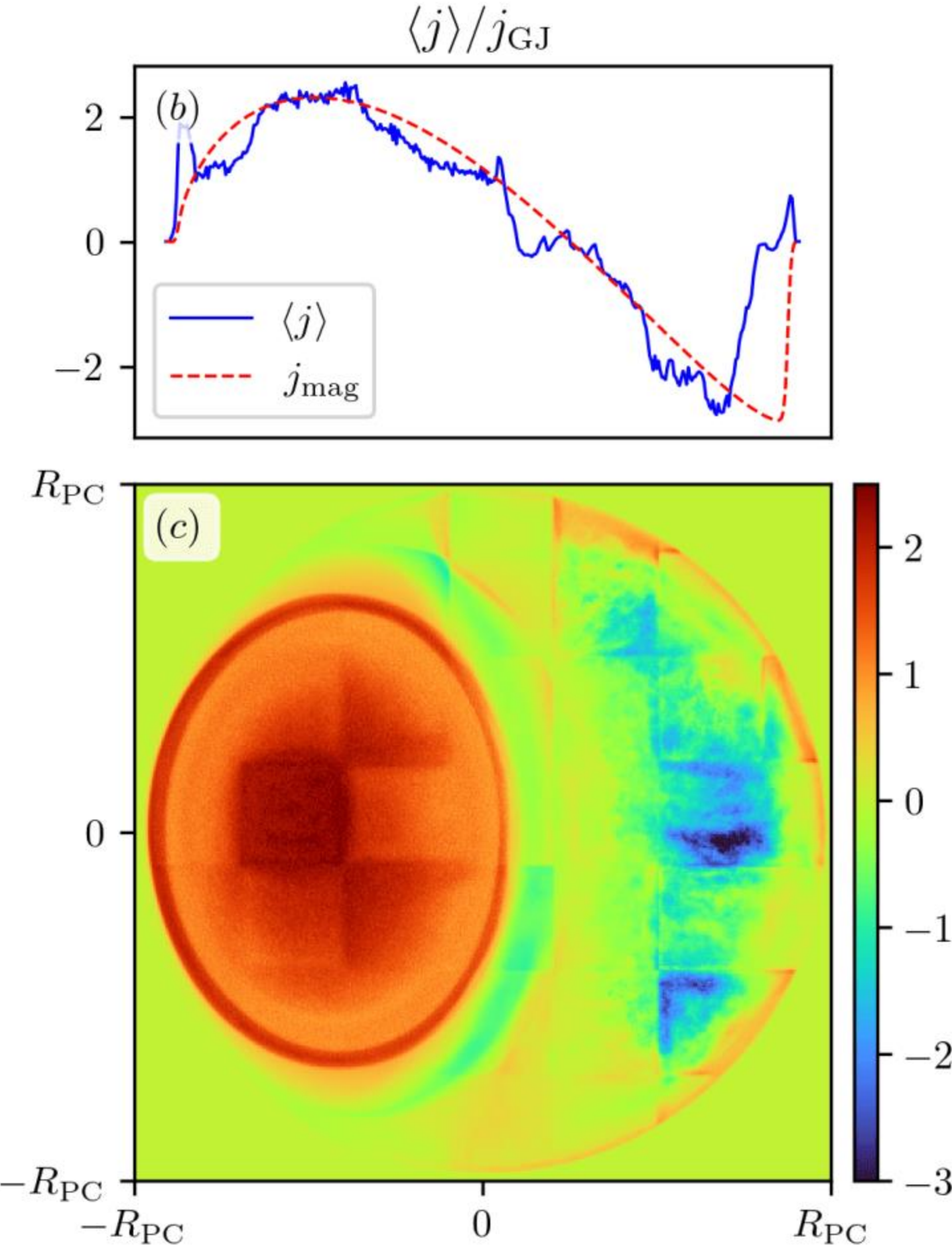
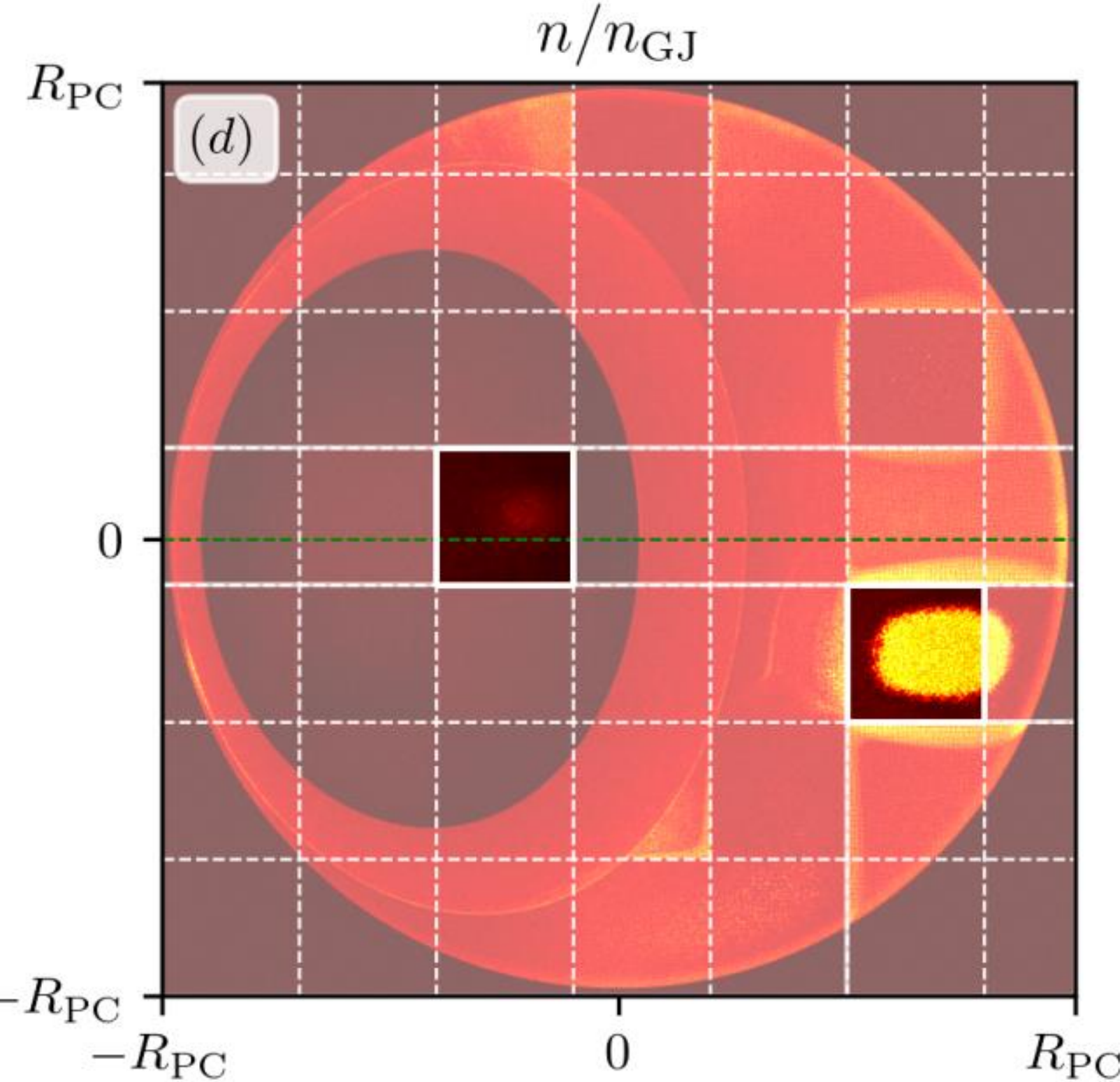


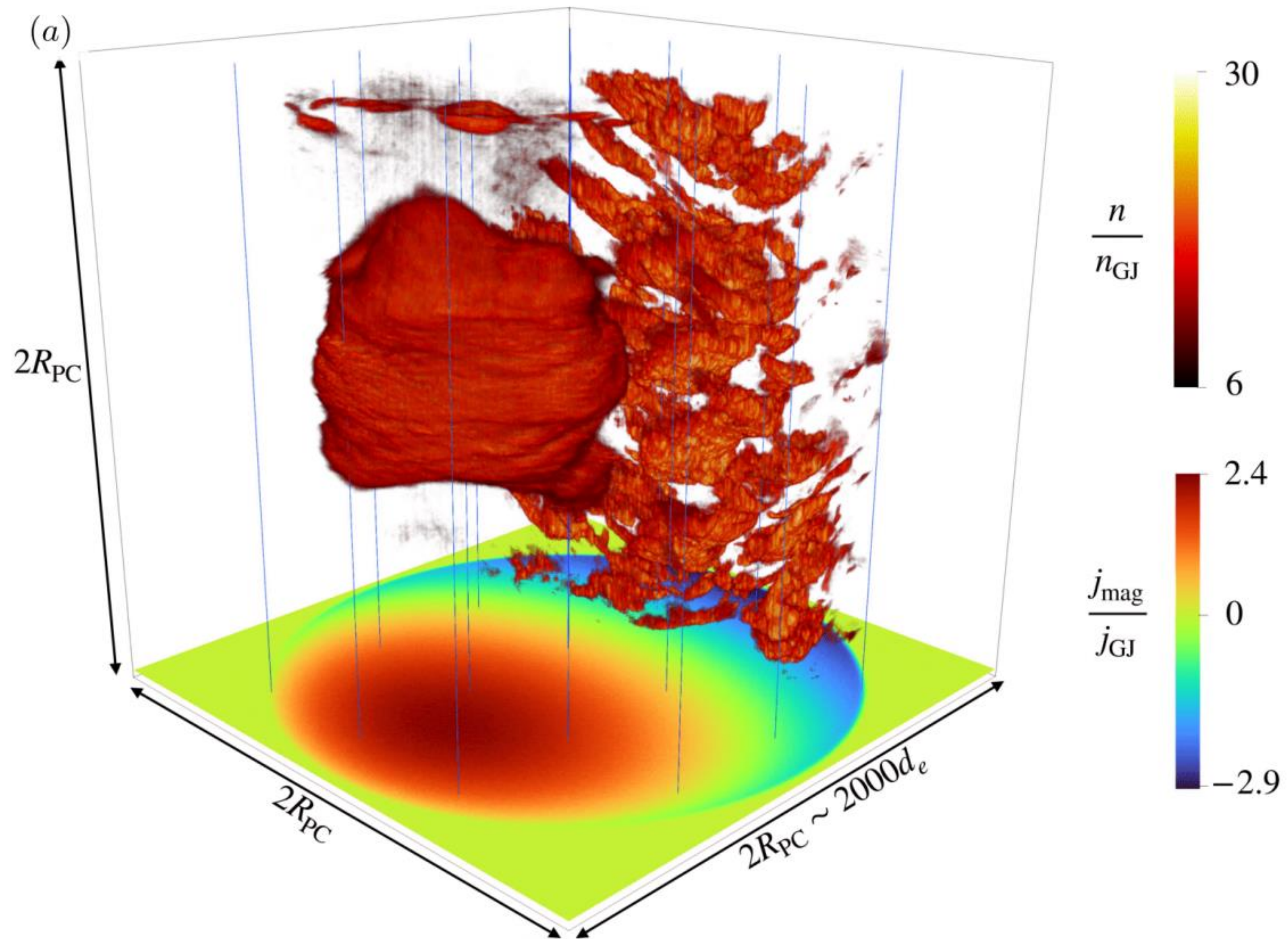
### (3) 3D, SCLF

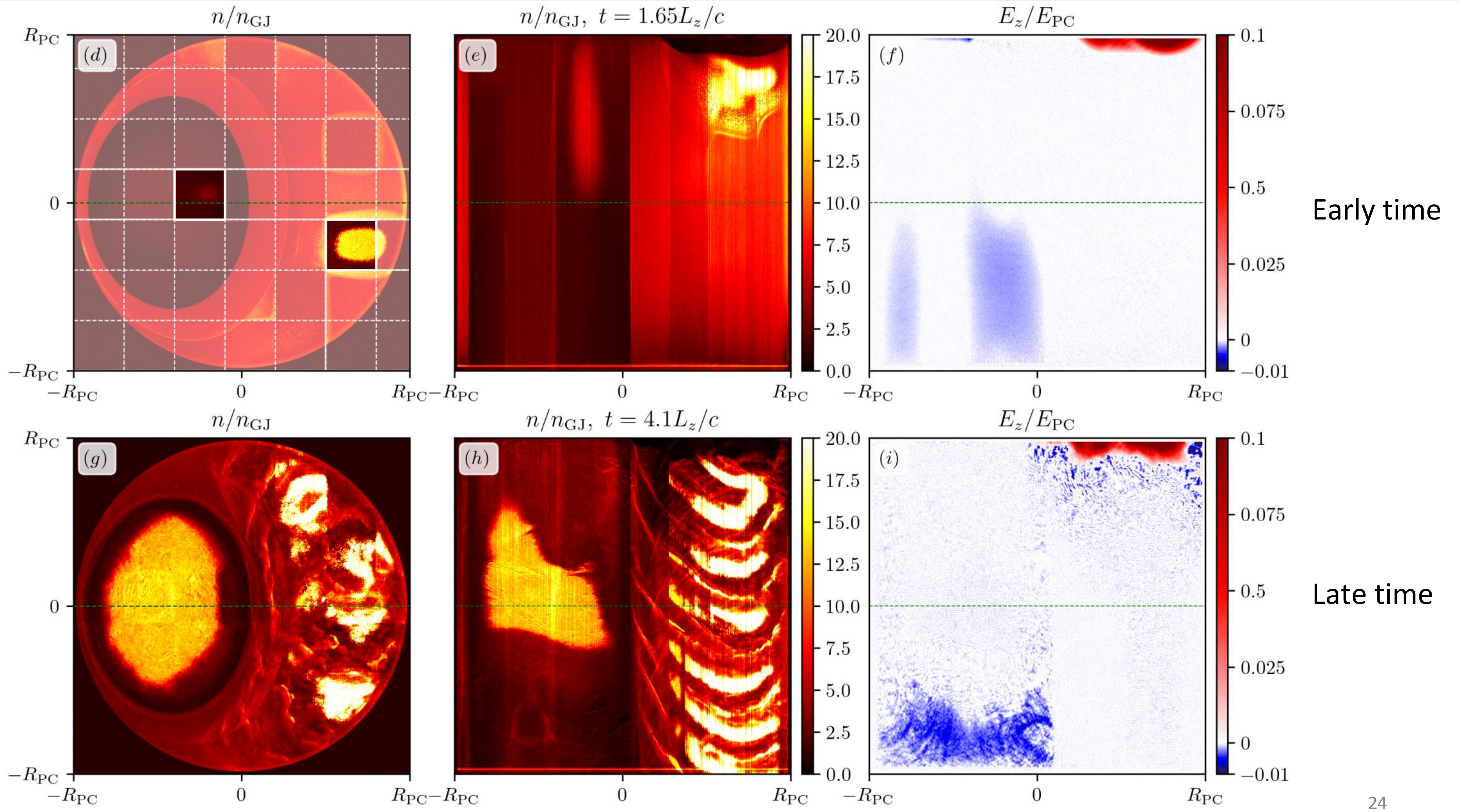
60° inclined rotator. Small gap for  $j/j_{GJ} < 0$ , larger gap for  $j/j_{GJ} > 1$ .

Divide polar cap into 6x6 square patches. Two patches with initial plasma injection.

Particle number density:





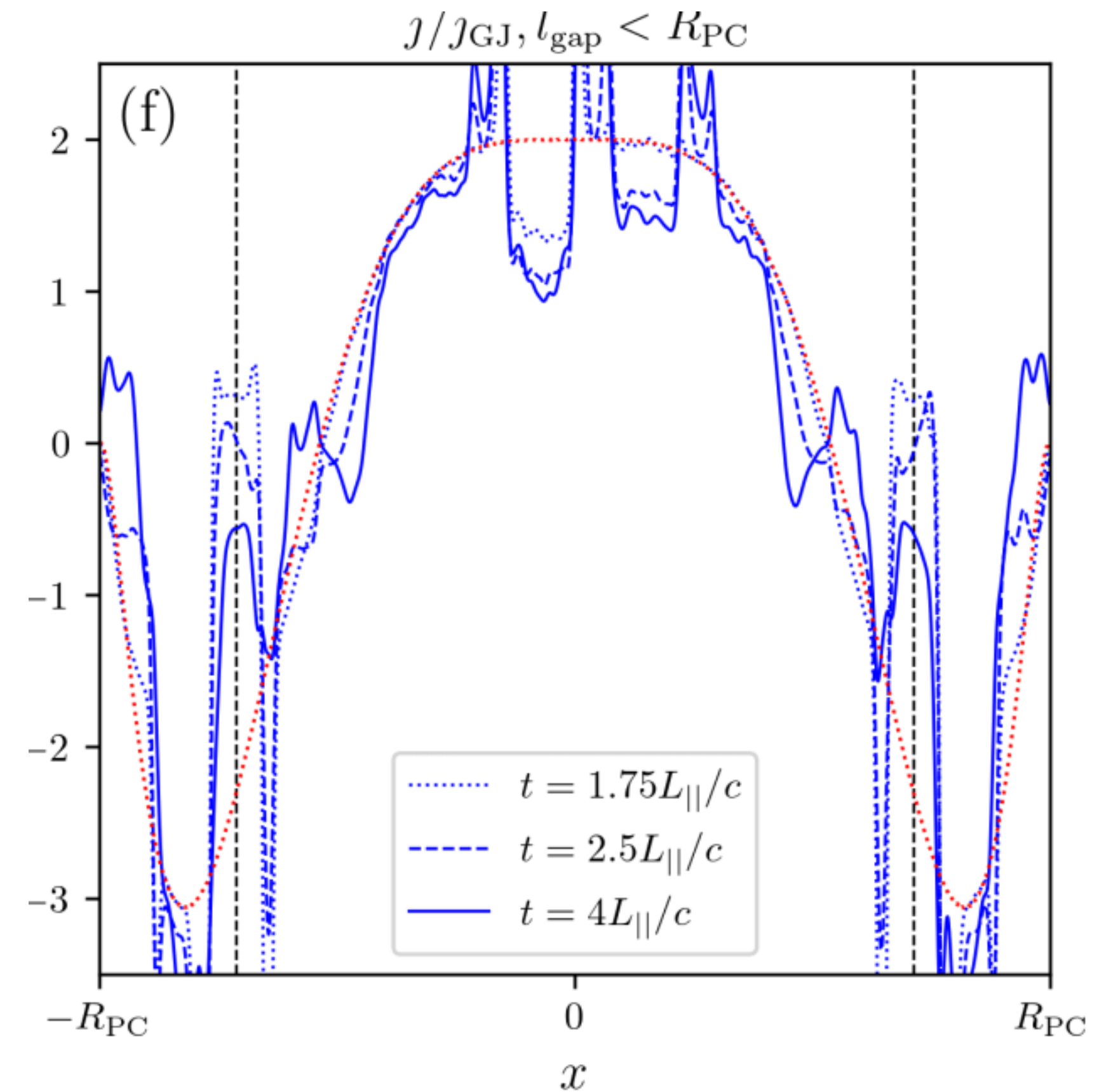
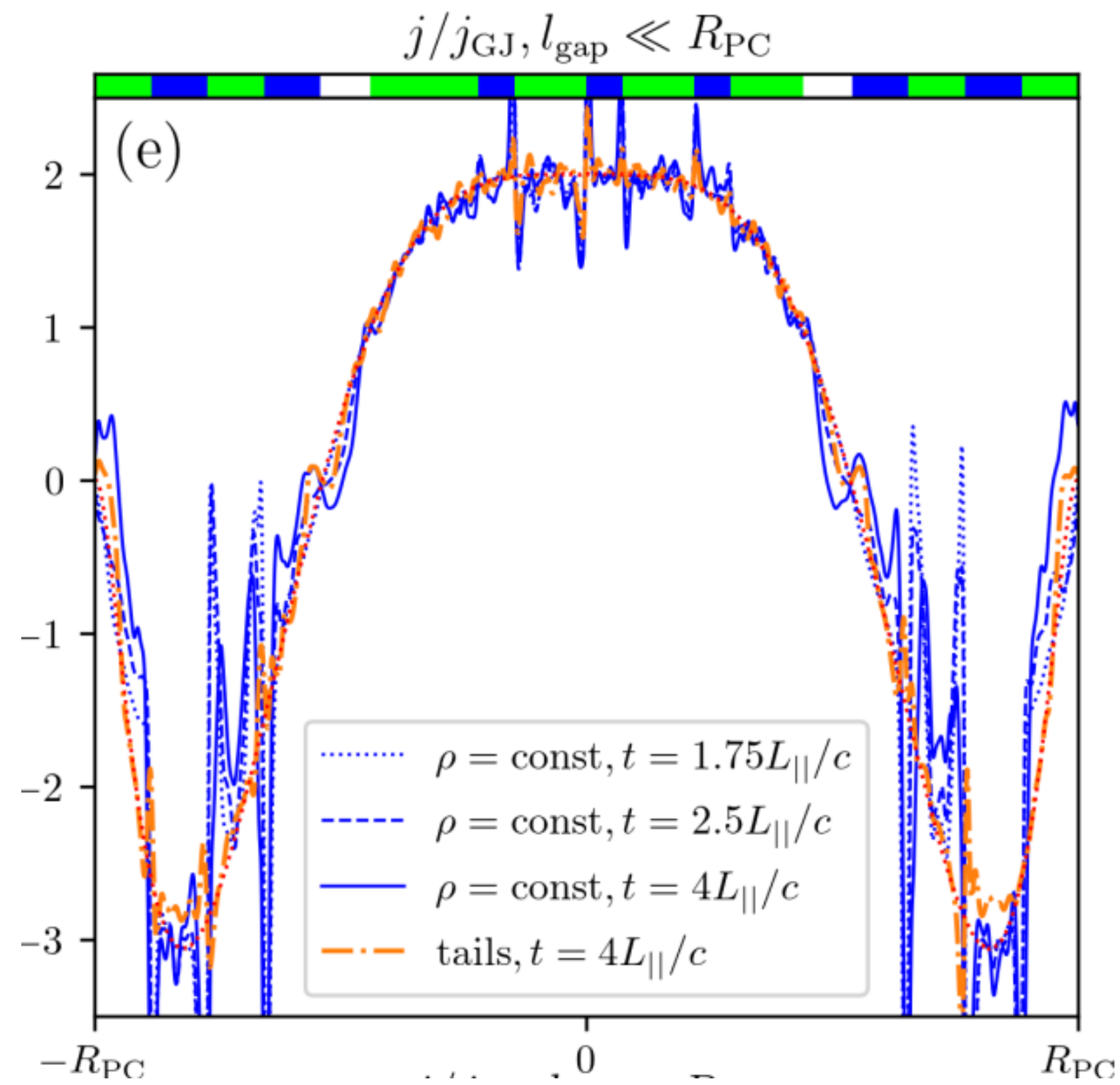




# (4) Check for the model validity: evolution of magnetic field twist

↔ evolution of magnetospheric current

Large gaps lead to a noticeable untwist of the field lines.



# IV. Conclusion & Discussion

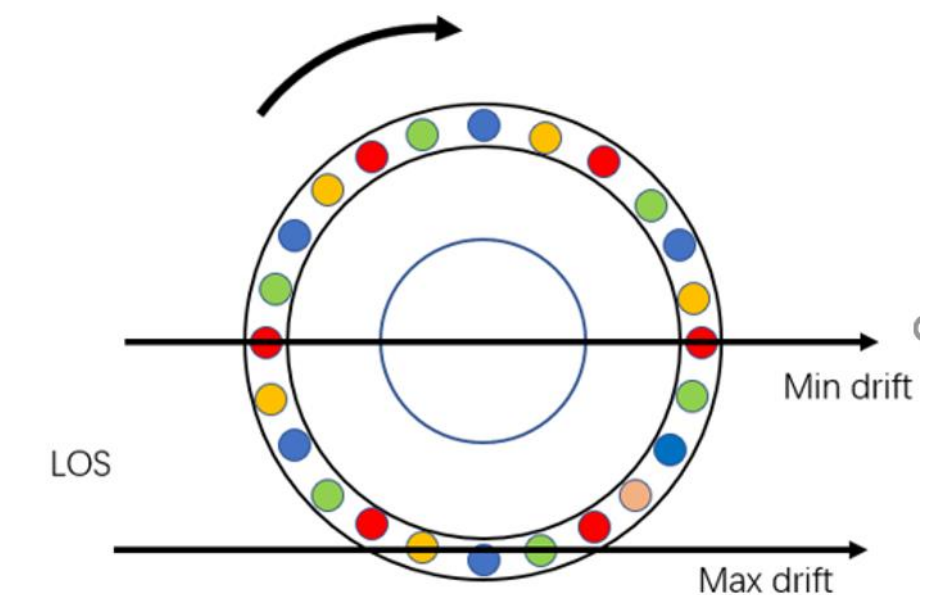
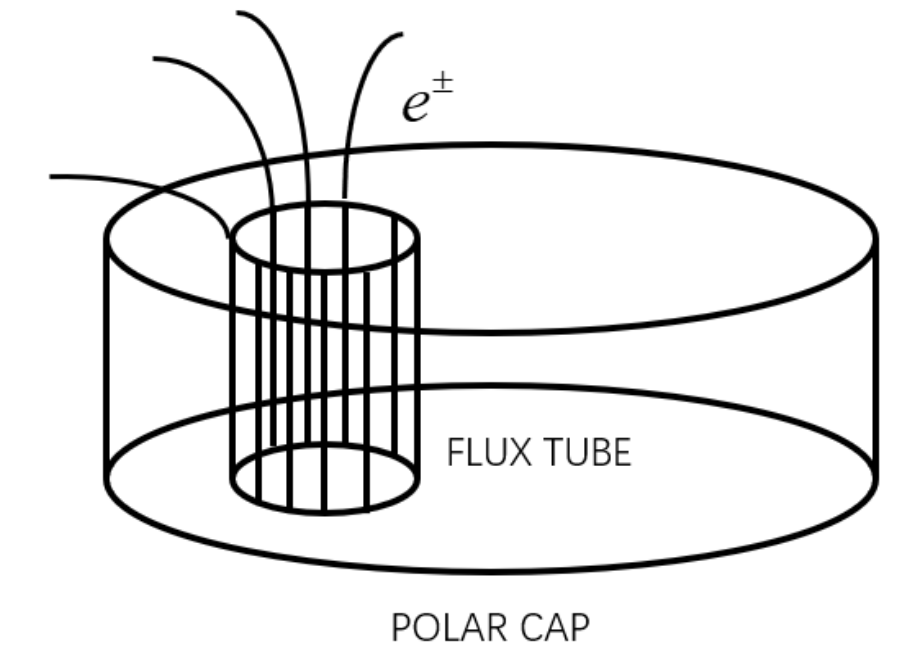
Main conclusion: transverse coherence scale of a discharge zone  $\sim$  longitudinal gap size

Discussion point 1: **NO spark.**

Polar caps are filled with discharge regions.  
NO noticeable plasma drifting.

Single pulse timescale  $\gg$  discharge timescale

Single pulse modulation  $\leftarrow$  Radiation happens at discharge boundaries?



Discussion point 2: for old pulsars, plasma density may be smaller → deviate from FFE.  
→ may have different properties from this paper's simulation.  
Larger gap → significant twist (at light cylinder) evolution  
→ larger timescale evolutions  
→ nulling... in old pulsars?

Discussion point 3: repetition rate of discharge... too artificial?

看完文章后我的观点:

(1) 本文模拟中, 放电过程本身对于RS模型和SCLF模型来说差别不大, 但它们在 $j/j_{GJ} > 1$ 的区域, 或者说核区, 的电场强度有明显差异。对于核区和环区的比较是一件可能值得干的事情, 能够鉴别模型。

(2) 本文的结论不支持spark存在, 但对于更复杂的脉冲星表面情形, spark是否可能存在?

(3) 对于年老和年轻脉冲星, 在观测数据分析上的更细致的比较是有意义的。年老脉冲星磁层偏离FFE, 在偏振上会有什么更显著的后果吗?

感谢大家 Thanks for your attention.